Circulation
JOURNAL OF THE AMERICAN HEART ASSOCIATION

Podoplanin-Expressing Cells Derived From Bone Marrow Play a Crucial Role in Postnatal Lymphatic Neovascularization

Ji Yoon Lee, Changwon Park, Yong Pil Cho, Eugine Lee, Hyongbum Kim, Pilhan Kim, Seok H. Yun and Young-sup Yoon

Circulation 2010;122;1413-1425; originally published online Sep 20, 2010;
DOI: 10.1161/CIRCULATIONAHA.110.941468
Circulation is published by the American Heart Association. 7272 Greenville Avenue, Dallas, TX 72514
 Print ISSN: 0009-7322. Online ISSN: 1524-4539

Podoplanin-Expressing Cells Derived From Bone Marrow Play a Crucial Role in Postnatal Lymphatic Neovascularization

Ji Yoon Lee, MS*; Changwon Park, PhD*; Yong Pil Cho, MD, PhD; Eugine Lee, MS; Hyongbum Kim, MD, PhD; Pilhan Kim, PhD; Seok H. Yun, PhD; Young-sup Yoon, MD, PhD

Background—Emerging evidence has suggested a contribution of bone marrow (BM) cells to lymphatic vessel formation; however, the exact phenotype of the cells with lymphatic endothelial progenitor cell function has yet to be identified. Here, we investigate the identity of BM-derived lymphatic endothelial progenitor cells and their role in lymphatic neovascularization.

Methods and Results—Culture of BM-mononuclear cells in the presence of vascular endothelial growth factors A and C and endothelial growth factor resulted in expression of lymphatic endothelial cell markers. Among these cells, podoplanin$^+$ cells were isolated by magnetic-activated cell sorting and characterized by fluorescence-activated cell sorter analysis and immunocytochemistry. These podoplanin$^+$ cells highly express markers for lymphatic endothelial cells, hematopoietic lineages, and stem/progenitor cells; on further cultivation, they generate lymphatic endothelial cells. We further confirmed that podoplanin$^+$ cells exist in small numbers in BM and peripheral blood of normal mice but are significantly (15-fold) augmented on lymphangiogenic stimuli such as tumor implantation. Next, to evaluate the potential of podoplanin$^+$ cells for the formation of new lymphatic vessels in vivo, we injected culture-isolated or freshly isolated BM-derived podoplanin$^+$ cells into wound and tumor models. Immunohistochemistry demonstrated that the injected cells were incorporated into the lymphatic vasculature, displayed lymphatic endothelial cell phenotypes, and increased lymphatic vascular density in tissues, suggesting lymphvasculogenesis. Podoplanin$^+$ cells also expressed high levels of lymphangiogenic cytokines and increased proliferation of lymphatic endothelial cells during coculture, suggesting a lymphangiogenic or paracrine role.

Conclusions—Our results provide compelling evidence that BM-derived podoplanin$^+$ cells, a previously unrecognized cell type, function as lymphatic endothelial progenitor cells and participate in postnatal lymphatic neovascularization through both lymphvasculogenesis and lymphangiogenesis. **(*Circulation*. 2010;122:1413-1425.)**

Key Words: bone marrow ■ lymphangiogenesis ■ lymphatic vessels ■ Gp38 protein, mouse ■ podoplanin protein, mouse

Lymphatic vessels play an important role in the pathogenesis of diseases such as lymphedema and tumors,[1,2] and an understanding of lymphatic biology is crucial to develop strategies to prevent or treat these diseases. Investigation of lymphatic vascular growth was made possible by the discovery of specific markers for lymphatic endothelial cells (LECs). The establishment of the lymphatic vasculature during mouse embryogenesis begins with expression of homeobox transcriptional factor PROX-1 in a subset of the venous endothelial cells of the cardinal vein[3] that express vascular endothelial growth factor (VEGF) receptor (VEGFR)-3[4] and LYVE-1.[5] Subsequently, the PROX-1–expressing (PROX-1$^+$) cells migrate out to form the primary lymphatic plexus, which undergoes further remodeling to form a mature network of LECs that express other LEC markers such as podoplanin (pod).[6,7] Pod is a 38-kDa integral membrane mucoprotein that is expressed predominantly in the endothelium of lymphatic capillaries.[7] Mice deficient in *pod* die at birth as a result of respiratory failure accompanied by malfunctioning lymphatic, but not blood, vessels with impaired lymphatic transport and congenital lymphedema.[8]

Clinical Perspective on p 1425

The generation of lymphatic vessels in adults was previously believed to be achieved exclusively by a process called lymphangiogenesis, the formation of new lymphatic vessels from preexisting lymphatic vasculature.[9–13] However, emerging evidence has suggested that lymphvasculogenesis may

Received January 27, 2010; accepted July 20, 2010.

From the Division of Cardiology, Department of Medicine, Emory University School of Medicine, Atlanta, Ga (J.Y.L., C.P., E.L. H.K., Y.-S.Y.); Department of Vascular Surgery, Asan Medical Center, University of Ulsan College of Medicine, Seoul, Korea (Y.P.C.); and Harvard Medical School and Massachusetts General Hospital, Wellman Center for Photomedicine, Boston, Mass (P.K., S.H.Y.). Dr Park is now at the Washington University School of Medicine, St Louis, Mo.

*Drs Lee and Park contributed equally to this article.

The online-only Data Supplement is available with this article at http://circ.ahajournals.org/cgi/content/full/CIRCULATIONAHA.110.941468/DC1.

Correspondence to Young-sup Yoon, MD, PhD, Division of Cardiology, Department of Medicine, Emory University School of Medicine, 1639 Pierce Dr, WMB 3009, Atlanta, GA 30322. E-mail yyoon5@emory.edu

Circulation **is available at http://circ.ahajournals.org** **DOI: 10.1161/CIRCULATIONAHA.110.941468**

also occur through putative progenitor cells for LECs. Studies have shown that bone marrow (BM) contains cells with the potential to generate LECs.[14–17] An early study reported that human fetal liver-derived, nonadherent $CD34^+CD133^+$ $VEGFR\text{-}3^+$ cells, when cultured, became adherent and expressed LYVE-1 or pod, implying a role for these cells as common blood vascular and lymphatic endothelial progenitor cells (LEPCs).[14] Using a chimeric mouse model in which BM of wild-type mice was reconstituted by BM transplantation from donor green fluorescent protein (GFP) mice, Religa and colleagues[16] subsequently showed that BM-derived cells were incorporated into newly formed lymphatic vessels in corneas. Maruyama and colleagues demonstrated incorporation of mouse GFP-BM cells into lymphatic vessels in inflamed corneas.[15] This study showed that tissue-resident $CD11b^+$ macrophages, presumably derived from BM, were incorporated into inflammation-induced lymphatics in the cornea. Kerjaschki et al[17] demonstrated the presence of male recipient-derived LECs in the lymphatic vessels in kidneys transplanted from female donors. Together, these studies support the idea that a certain population of BM cells, likely of monocyte-macrophage lineages, can give rise to LECs in the foci of new lymphatic vessel formation (lymphatic neovascularization) in various pathological conditions. However, no studies have clearly addressed the exact identity of BM-derived LEPCs in adults and tested their potential for lymphatic neovascularization by external implantation of isolated LEPCs.

In this study, we show for the first time that pod^+CD11b^+ cells exist in adult BM and can function as LEPCs. We also demonstrate that these cells contribute to lymphatic neovascularization through dual lymphvasculogenic and lymphangiogenic roles.

Methods

All protocols for animal experiments were approved by the Institutional Animal Care and Use committees of Emory University.

Culture of BM Mononuclear Cells

Mouse BM mononuclear cells (MNCs) fractionated by density gradient centrifugation with Histopaque-1083 (Sigma, St Louis, Mo) were seeded onto 100-mm culture dishes coated with rat vitronectin. To optimize culture conditions to generate LEPCs, 4 different combinations of media were used (Table I in the online-only Data Supplement). To differentiate sorted putative LEPCs derived from cultured BM-MNCs into LECs, the cells were maintained in endothelial cell basal medium-2 (EBM-2) supplemented with cytokine cocktail (SingleQuots; Lonza (San Diego, Calif) for 7 days.

LEC Proliferation Assay

The sorted pod^+ and pod^- cells (2.5×10^3) from BM-MNCs cultured for 4 days were mixed with human dermal LECs (1.5×10^4; Cambrex, East Rutherford, NJ) that were prelabeled with CM-Dil (Invitrogen, Carlsbad, Calif), seeded onto 96-well culture plates, and cocultured in endothelial cell growth medium media with 1% FBS. Twenty-four hours later, cells were stained with Ki67 antibody and counterstained with DAPI. Cells positive for Dil, Ki67, and DAPI were counted.

Mouse Cornea Model

A micropocket was created, followed by implantation of a micropellet containing VEGF-C and fibroblast growth factor-2.[18] Subsequently, CM-Dil–labeled pod^+ cells cultured for 4 days were injected into the surrounding area in the cornea. Eyeballs were isolated 7 days later and subjected to immunohistochemistry.

Skin and Ear Wound Models

After creating full-thickness excisional skin wounds on the backs or ears of the mice, we injected pod^+ cells labeled with DiI or derived from GFP mice into the wound bed around the wound. Seven days later, the wound tissues, including a perimeter of 1 to 2 mm of normal skin tissue, were harvested for immunohistochemistry.

Mouse Tumor (Melanoma) Model

Tumor cells (B16-F1 melanoma cell line) were subcutaneously injected into the middle dorsum of C57BL/6 mice. Seven days later, Dil-labeled pod^+ cells isolated from cultured BM-MNCs were injected into the tumor vicinity, and the mice were euthanized 7 days later for immunohistochemistry.

Measurement of Lymphatic Capillary Density

After implantation of tumors (melanomas) and injection of pod^+ cells, pod^- cells, or the same volume of PBS as described above, tumors and surrounding peritumoral tissues with skin were harvested and subjected to immunohistochemistry with a VEGFR-3 antibody.[19] Lymphatic capillary density was calculated from at least 10 randomly selected fields.

Statistical Analysis

All results are presented as mean±SE. Statistical analyses were performed with the Mann–Whitney *U* test for comparisons between 2 groups and the Kruskal-Wallis ANOVA test for >2 groups. Values of $P\leq0.05$ were considered to denote statistical significance. Details on the above and other methods can be found in the online-only Data Supplement.

The authors had full access to and take full responsibility for the integrity of the data. All authors have read and agree to the manuscript as written.

Results

BM-MNCs Cultured Under Defined Conditions Express LEC Markers

To explore whether BM-MNCs include potential LEPCs, we first examined LEC marker expression in freshly isolated BM-MNCs of FVB mice by quantitative reverse-transcriptase polymerase chain reaction (qRT-PCR). Uncultured BM-MNCs expressed *Cd31* and *Lyve1* but not *Prox1, Vegfr3*, or *pod* (Figure 1A). Next, to investigate whether culture of BM-MNCs under defined conditions can induce LEC gene expression, we cultured BM-MNCs in EBM-2 supplemented with VEGF-A, VEGF-C, and epidermal growth factor (EGF) individually or in various combinations (Table I in the online-only Data Supplement). We selected VEGF-A and VEGF-C because of their known role as lymphatic growth factors[11,20] and EGF because of its role in cell proliferation.[21] Expression of *Prox1* and *Vegfr3* emerged at day 1, reached a peak at day 4, and decreased but continued until day 7. *Pod* expression went up from day 1 and was sustained until day 10; *Cd31* and *Lyve1* expression decreased over the 4 days (Figure 1A). Another lymphatic marker, *Foxc2,* was also expressed in the VEGF-A, VEGF-C, and EGF (ACE) condition with a peak at day 4 (data not shown). From these experiments, we found that cultivation of BM-MNCs with lymphangiogenic factors can generate LEC-like cells. We further found that 4-day culture under the ACE condition was optimal for generating LEC-like cells because all the LEC markers were significantly expressed whereas expression of a pan–vascular endothelial cell marker, *Cd31*, was significantly reduced at day 4. Immunocytochemistry and fluorescence-ac-

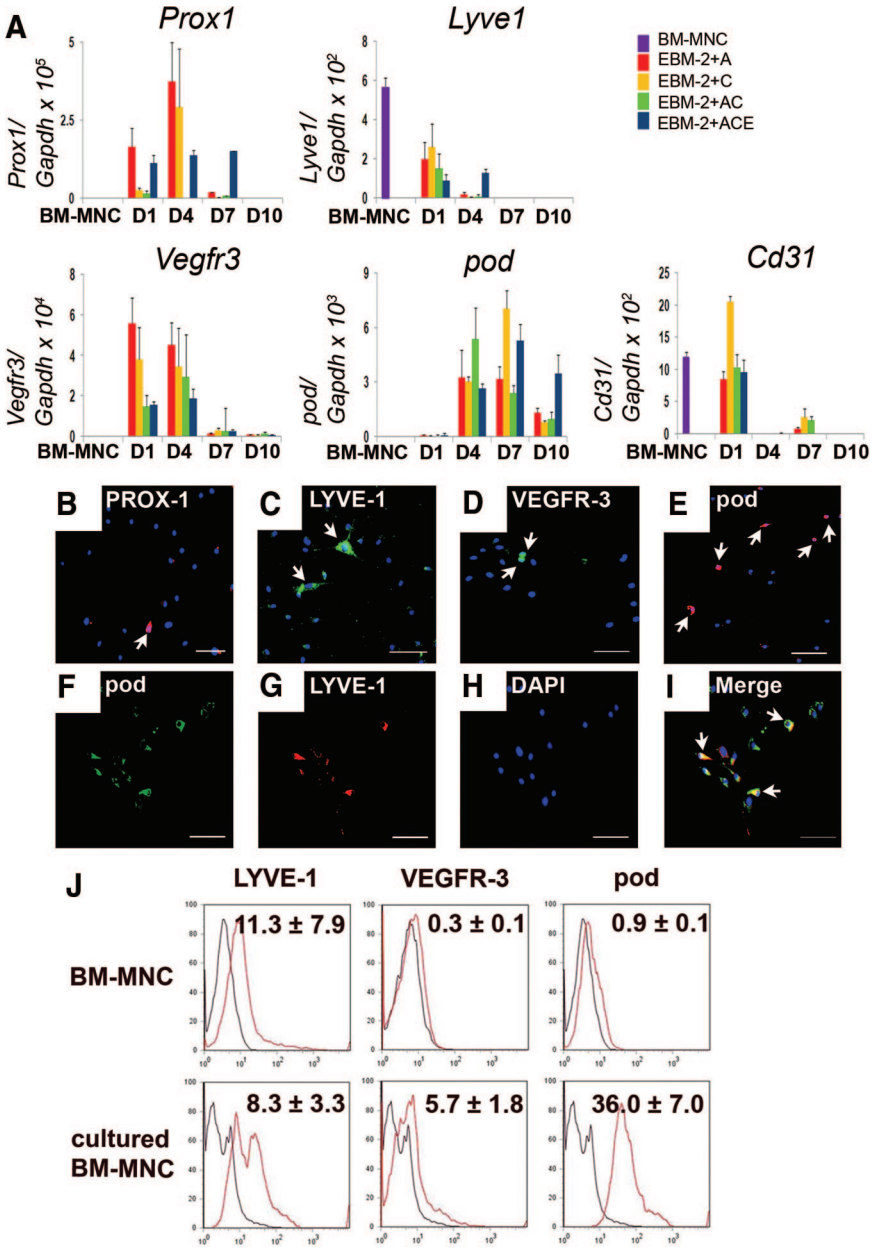

Figure 1. Expression of LEC markers in BM-MNCs cultured with lymphangiogenic cytokines. A, BM-MNCs were cultured under various culture conditions; harvested at day 1, 4, 7, or 10; and subjected to qRT-PCR. Each value is the average of 3 independent experiments (n=4 per experiment). A, VEGF-A; C, VEGF-C; E, EGF. B through J, Expression of LEC markers in BM-MNCs that were cultured for 4 days under the ACE condition. Immunocytochemistry (B through I): DAPI (blue) for nuclear staining. I, Merged image of images in F through H; scale bar=100 μm. J, FACS analysis. Numbers in boxes are the percentages of cells positive for the indicated proteins. Each value is the average of 3 independent experiments (n=4 per experiment).

tivated cell sorter (FACS) analysis also confirmed the qRT-PCR results (Figure 1B and 1J). FACS analyses showed a significant increase in pod$^+$ and VEGFR-3$^+$ cells and similar levels of LYVE-1$^+$ cells in cultured BM-MNCs compared with the freshly isolated BM-MNCs (Figure 1J). The expression levels of LEC markers in the pod$^+$ cells were similar to those of mouse LECs isolated from a mouse EC line, SVEC4–10+ (Figure I in the online-only Data Supplement). Taken together, these results indicate that culture of BM-MNCs under the ACE condition can generate cells expressing LEC markers. We therefore used this culture condition for the following experiments.

Pod$^+$ Cells Isolated From Cultured BM-MNCs Express LEC Markers, Hematopoietic and Stem/Progenitor Cell Markers, and Lymphangiogenic Cytokines

Because these cultured cells were still heterogeneous, we next sought to enrich cells with the LEC phenotype using a cell sorting strategy. Among the 3 representative LEC surface markers, LYVE-1, VEGFR-3, and pod, we selected pod on the basis of the qRT-PCR data (Figure 1A), which showed pod expression to be the most stable from day 4 on. Pod has been implicated in proper patterning of lymphatic vessels and lymphedema.[7,8] Accordingly, we isolated pod$^+$ or pod$^-$ cells from the cultured BM-MNCs at day 4 by a magnetic-activated cell sorting and examined the LEC markers. qRT-PCR analysis demonstrated augmented expression of *Prox1* (3.7-fold), *Lyve1* (3.0-fold), and *pod* (6.0-fold) in the pod$^+$ fraction compared with the pod$^-$ fraction (Figure 2A). *Vegfr3* expression was slightly higher in the pod$^+$ than the pod$^-$ cells. However, pod$^+$ cells showed lower expression of *Cd31* (3.6-fold). qRT-PCR analysis further revealed that representative lymphangiogenic cytokines such as *Vegfa* (2.1-fold), *Vegfc* (3.8-fold), *Vegfd* (6.8-fold), *Igf1* (8.9-fold), *Ang1* (4.8-fold), *Hgf* (48.1-fold), and *bFgf* (14.4-fold) were expressed

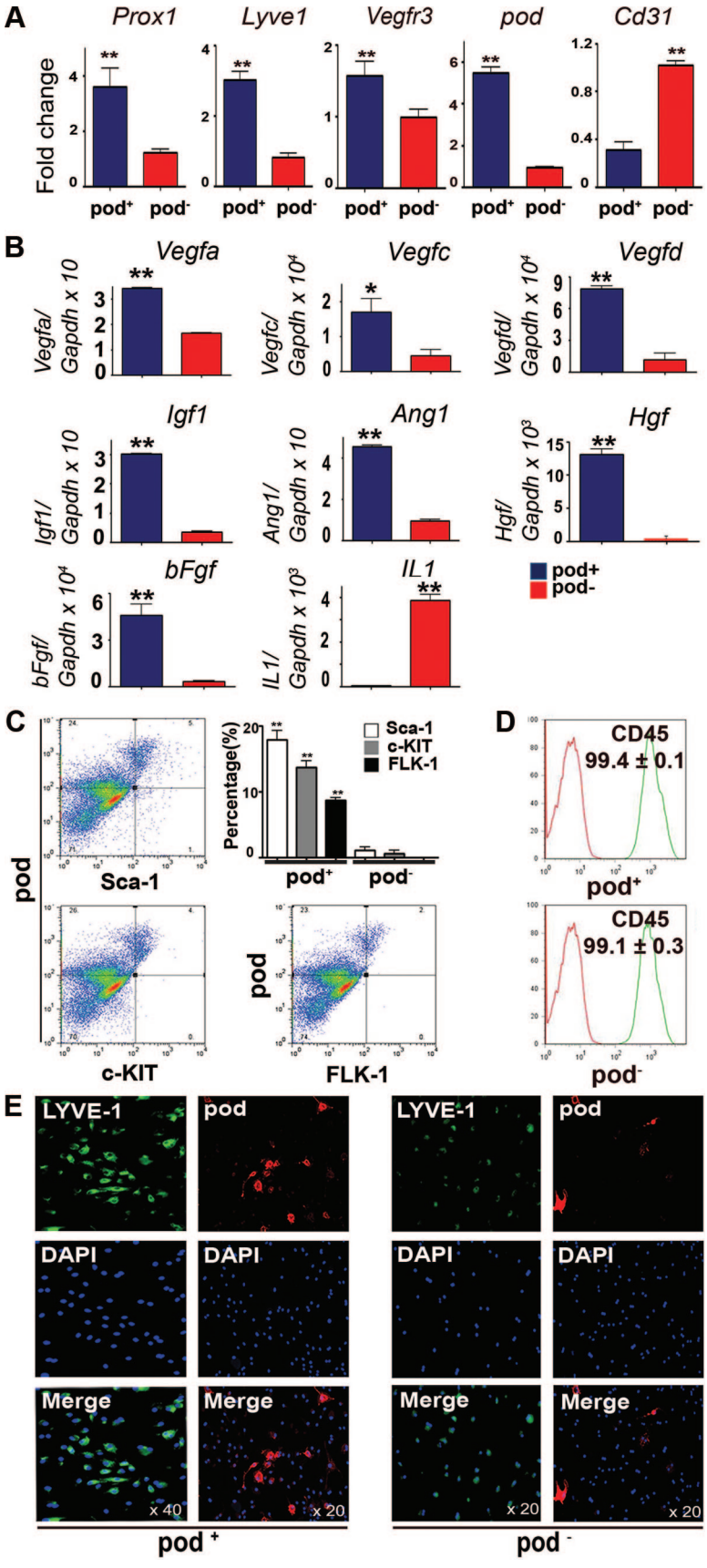

Figure 2. Enriched expression of lymphangiogenic cytokines and markers for LECs and HSCs in the culture-isolated pod$^+$ cells. A through D, The magnetic-activated cell–sorted pod$^+$ and pod$^-$ cells from 4 day-cultured BM-MNCs were subjected to qRT-PCR (A, B) and FACS analysis (C and D). Each value is the average of 3 independent experiments (**$P<0.01$, *$P<0.05$; n=4 per experiment). E, The sorted cells were further cultured for 7 days and subjected to immunocytochemistry for LYVE-1 and pod.

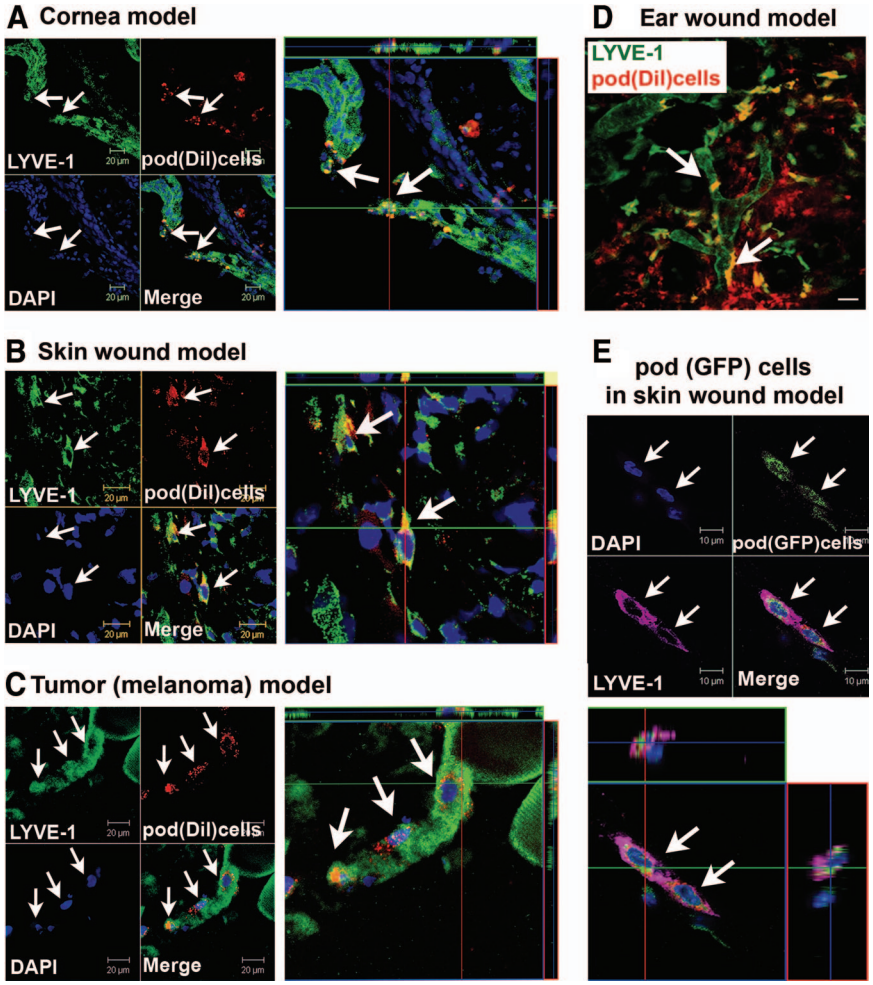

Figure 3. Lymphvasculogenesis from pod$^+$ cells in animal models. A through C, Mice that had received surgery for cornea micropocket, wound, or implantation of tumor cells (B16–F1 Melanoma) were injected with DiI-labeled pod$^+$ cells (red), and the tissues were harvested 7 days later for immunohistochemistry. A through C, Representative confocal images from cornea (A), wounded skin (B), and peritumoral subcutaneous tissues (C) demonstrated that DiI-labeled pod$^+$ cells were incorporated into lymphatic vessels and exhibited an LEC marker, LYVE-1. D, In vivo live confocal microscopic image from an ear wound model showed that multiple pod$^+$ cells (DiI) were clearly incorporated into lymphatic vessels and colocalized with LYVE-1. Arrows indicate cells positive for DiI and LYVE-1. Scale bar=20 μm. E, Skin wound tissues injected with pod$^+$ cells from GFP mice were stained for LYVE-1 and examined by confocal microscopy. Injected pod$^+$ GFP cells (arrows) were incorporated into the lymphatic vessels and expressed LYVE-1. Representative images from at least 2 independent experiments for each animal model are shown (n=3 per experiment). Scale bar=10 μm. Blue fluorescence indicates DAPI.

more highly in pod$^+$ cells than pod$^-$ cells, implying more potent paracrine lymphangiogenic activity of pod$^+$ cells (Figure 2B)[2,23,24] Next, we examined the progenitor character of pod$^+$ cells. FACS analysis showed that the hematopoietic stem cell markers Sca-1, c-KIT, and FLK-1 were expressed in 17.8±3.4%, 13.6±2.4%, and 8.6±0.9% of the pod$^+$ cells, respectively (Figure 2C). In contrast, pod$^-$ cells expressed virtually no hematopoietic stem cell markers. More than 99% of cultured pod$^+$ cells expressed CD45 (Figure 2D), indicating that these pod$^+$ cells are hematopoietic in origin and are not contaminating preexisting LECs from BM. Importantly, when further cultured for 7 days in conventional LEC culture media, which is EBM-2 supplemented with SingleQuots (complete EGM),[25] the pod$^+$ cells maintained expression of pod and LYVE-1, whereas pod$^-$ cells hardly expressed these markers (Figure 2E). We also found that the pod$^+$ cells have multilineage differentiation potential, as demonstrated by expression of markers of blood endothelial cells, smooth muscle cells, and fibroblasts, depending on culture conditions (Figure II in the online-only Data Supplement). Taken together, these findings indicate that pod$^+$ cells isolated from cultured BM-MNCs are enriched with LEC markers and lymphangiogenic cytokines, are hematopoietic in origin, possess stem/progenitor cell characteristics, and differentiate into LECs when further cultured, suggestive of putative LEPCs.

Culture-Isolated Pod$^+$ Cells Contribute to Lymphatic Vessel Formation in Animal Models

Next, we sought to determine the lymphatic neovascularization potential of these pod$^+$ cells. We thus injected pod$^+$ cells into 4 different animal models that are well known to induce lymphatic vessel formation: a corneal micropocket model[15] (Figure 3A), ear and skin wound models[26] (Figure 3B, 3D, and 3E), and a tumor (melanoma) model[27] (Figure 3C). Culture-isolated pod$^+$ cells prelabeled with DiI, a red fluorescent dye used for cell tracking, were injected into the margin of the cornea (cornea model) or into the subcutaneous tissues (wound models or tumor model). The tissues were harvested 7 days later and subjected to immunohistochemistry. Three-dimensional reconstruction of the confocal microscopic images demonstrated that pod$^+$ cells were clearly incorporated into lymphatic vessels and colocalized with cells expressing LEC markers in tissues harvested from all 4 models (Figure 3A through 3C and Movie I in the online-only Data Supplement). The percentage of the LYVE-1$^+$ lymphatic vessels containing DiI$^+$ cells was ≈5.2±2.1% in the cornea, 5.5±2.5% in wound models, and 8.5±3.7% in the tumor model. Of note, the Z-stacked, 3-dimensional images of Figure 3C (tumor model) unequivocally showed that pod$^+$ cells were incorporated into lymphatic vessels, exhibited a LEC marker, and had single nuclei, suggesting lymphvascu-

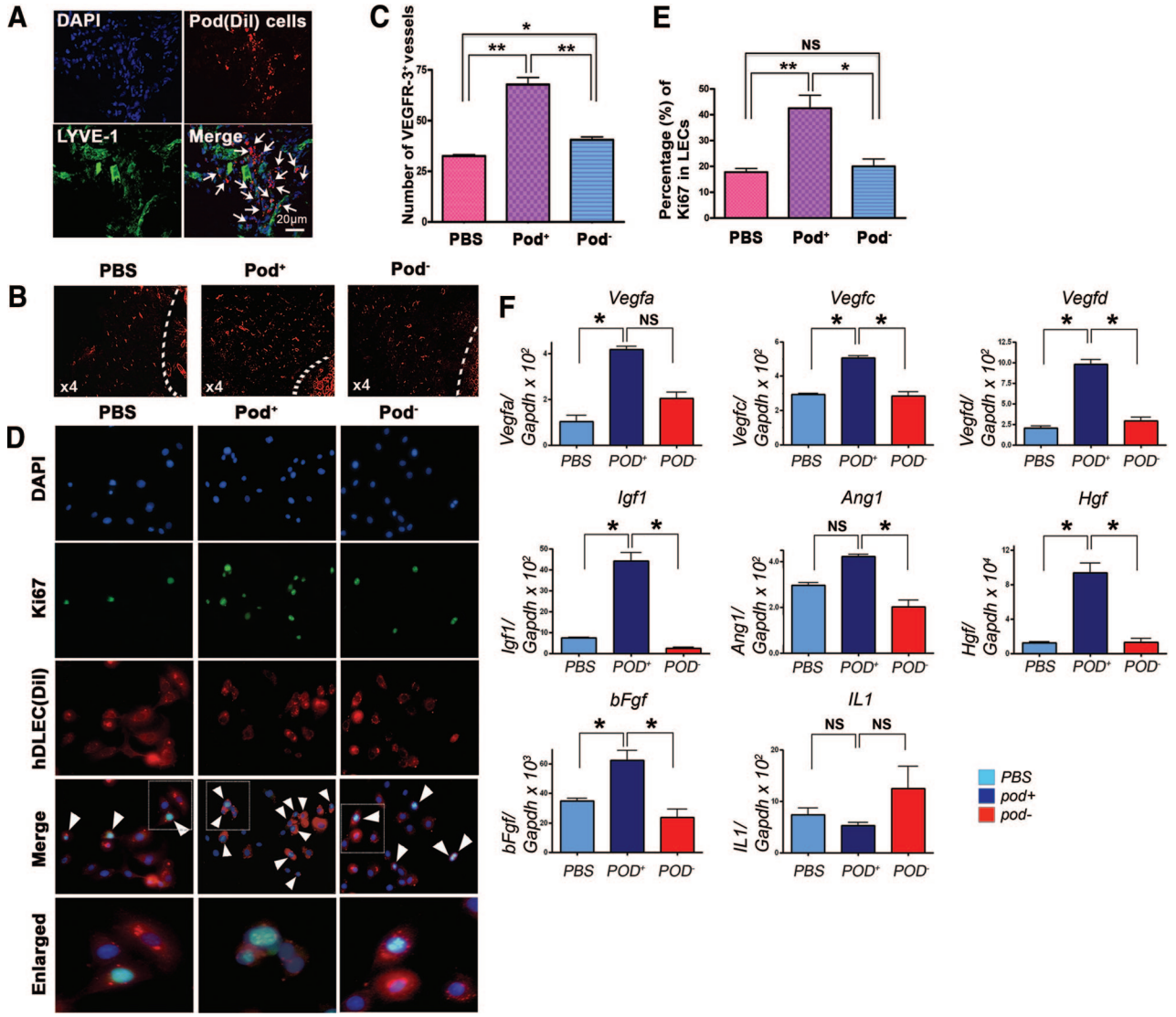

Figure 4. Lymphangiogenic characteristics of pod$^+$ cells. A, Pod$^+$ cells sorted from BM-MNCs cultured for 4 days labeled with DiI were injected into the periphery of tumors in mice that had been injected with melanoma cells 7 days before. Seven days after cell implantation, tumor and peritumoral tissues, including skin, were harvested and underwent immunostaining for LYVE-1 (green). Arrows indicate engraftment of pod$^+$ cells in close proximity to lymphatic vessels. Representative images from >2 independent experiments are shown (n=3 per experiment). DAPI is blue. Scale bar=20 μm. B, The peritumoral tissues that were injected with pod$^+$ cells, pod$^-$ cells, or the same volume of PBS as in the procedure described above were harvested 7 days later and subjected to immunohistochemistry with a VEGFR-3 antibody. Representative images from at least 2 independent experiments are shown (n=2 per group). Magnification ×4. C, The number of VEGFR-3$^+$ vessels in peritumoral tissues was higher in mice implanted with pod$^+$ cells than pod$^-$ cells or PBS. The indicated values were calculated from 2 independent experiments (B) using >10 randomly selected fields (**P<0.01, *P<0.05). D, The pod$^+$ and pod$^-$ cells from BM-MNCs cultured for 4 days or PBS were mixed with DiI-labeled human dermal LECs (hDLEC; red), cultured for 24 hours, and stained for Ki67 (green). DAPI is blue. The cells positive for DiI, Ki67, and DAPI (white arrowheads) were counted. Representative images from 3 independent experiments are shown. Scale bar=20 μm. E, Human dermal LECs cocultured with pod$^+$ cells exhibited a higher rate of Ki67$^+$ cells compared with controls, suggesting a lymphangiogenic role of pod$^+$ cells on surrounding LECs. The indicated values are the averages calculated from 14 randomly selected fields of each group of 3 independent experiments (**P<0.01, *P<0.05). F, Tissues from mice injected with pod$^+$ or pod$^-$ cells were subjected to qRT-PCR analyses. Graphs from 3 independent experiments are shown (*P<0.05; n=3 per group).

logenesis from the injected pod$^+$ cells. In addition, in vivo video-rate laser scanning microscopy demonstrated incorporation and colocalization of the injected pod$^+$ cells into LYVE-1$^+$ lymphatic vessels at multiple sites in the ear wound (Figure 3D) and cornea (data not shown) models. Immunohistochemistry further confirmed the incorporation of the injected cells into pod-expressing vessels, which displayed typical lymphatic vessel morphology (Figure III in the online-only Data Supplement). To complement these results with DiI-labeled pod$^+$ cells, we performed another experiment in which pod$^+$ cells culture-isolated from GFP mice were injected into a skin wound model (Figure 3E and Movie 2 in the online-only Data Supplement). Confocal microscopic imaging revealed that GFP$^+$ cells were incorporated into lymphatic vessels and expressed LYVE-1.

We also found that a larger portion of the injected cells were localized in close proximity to the lymphatic vasculature in the ear wound, tumor, and cornea models (Figures 3D

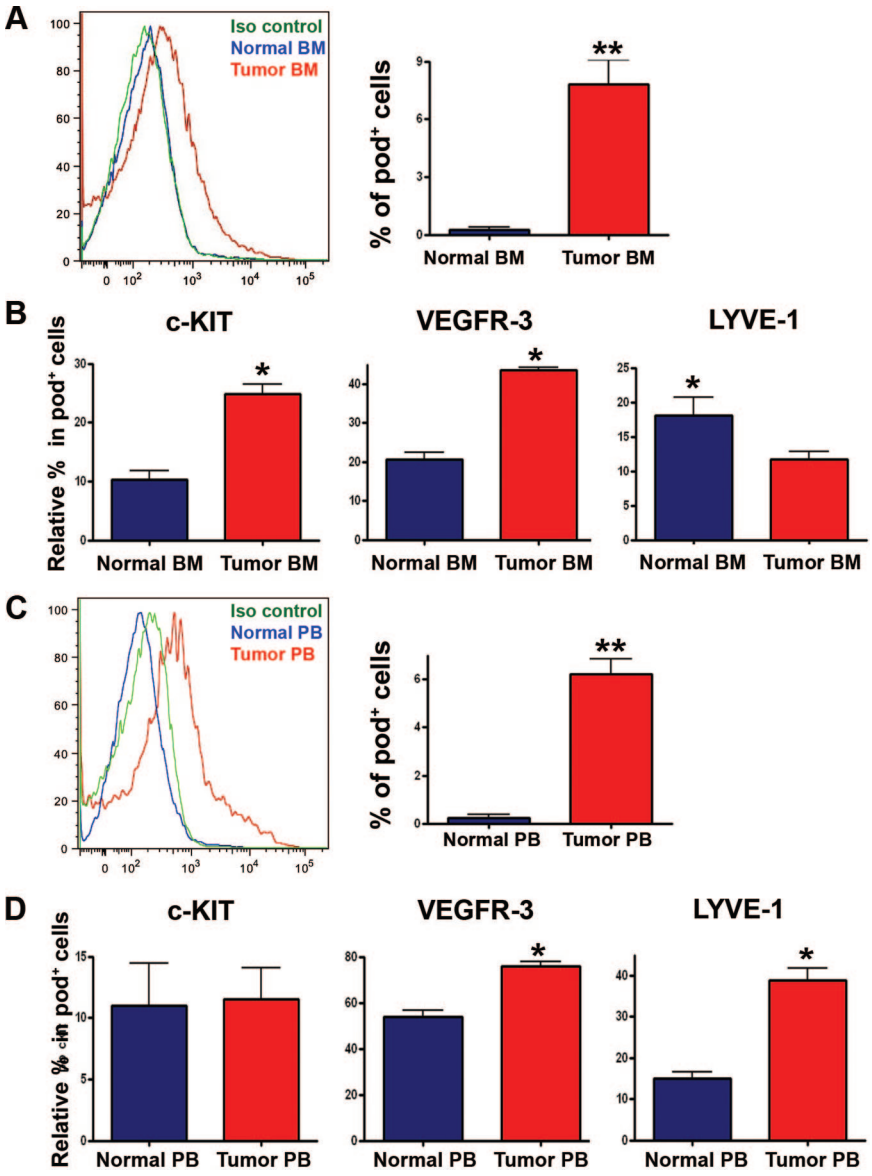

Figure 5. Augmentation of pod$^+$ cells in BM and PB on tumor induction. Cells prepared from BM (A and B) or PB (C and D) of normal or tumor (B16–F1 melanoma cells) -bearing mice were subjected to FACS analysis. Representative images from 3 independent experiments are shown (**$P<0.01$, *$P<0.05$; n=3 per group).

and 4A and Figure IV in the online-only Data Supplement), suggesting their lymphangiogenic role. To determine the overall lymphatic neovascularization potential of pod$^+$ cells, we measured lymphatic vascular density in peritumoral tissues and found that pod$^+$ cell–injected tissues showed significantly higher lymphatic vascular density than PBS- or pod$^-$ cell–injected tissues (Figure 4B and 4C). To further explore their lymphangiogenic role, we cocultured pod$^+$ cells with DiI-labeled human dermal LECs and determined the proliferation of LECs by Ki67 staining. The number of Ki67-positive LECs was >2-fold higher in the pod$^+$ cell–cocultured LECs than PBS-added or pod$^-$ cell–cocultured LECs (Figure 4D and 4E). In agreement with these data, lymphangiogenic cytokines in tissues measured at day 7 after injection of 2×10^6 pod$^+$ cells in the skin wound model were significantly increased in the pod$^+$ cell–injected mice compared with PBS- or pod$^-$ cell–injected tissues (Figure 4F). From these in vitro and in vivo studies, we concluded that culture-isolated pod$^+$ cells have dual lymphvasculogenic and lymphangiogenic roles and augment lymphatic neovascularization.

Pod$^+$ Cells Are Increased in BM and Peripheral Blood Under Lymphangiogenic Conditions, and Pod$^+$ Cells Contribute to Lymphatic Neovascularization

Next, we investigated whether pod$^+$ cells directly isolated from animals could function similarly to culture-driven pod$^+$ cells. Because only a small number of BM-MNCs are pod$^+$ in the steady-state normal animal (Figure 1J), we hypothesized that if these cells function as LEPCs, the number would be increased in the BM and/or peripheral blood (PB) under conditions promoting lymphatic vascular growth. Hence, we injected B16-F1 melanoma cells[27] subcutaneously into the backs of mice and examined the number of pod$^+$ cells in BM and PB 7 days later by FACS. FACS analysis showed that pod$^+$ cells in BM and PB were <0.5% in healthy C57/BL6 mice but increased ≈15-fold both in BM and PB on the

growth of melanoma (BM, 0.2±0.5% versus 3.2±1.0%; PB, 0.4±0.3% versus 6.7±2.0%; $P<0.01$; Figure 5A and 5C). Similar results were found in nude mice implanted with MDA-MB-231 human breast cancer cells (data not shown). Next, we examined the expression of VEGFR-3, LYVE-1, and c-KIT in pod$^+$ cells isolated from BM and PB of normal and tumor-bearing mice to determine the progenitor and lymphatic character of the pod$^+$ cells. FACS analysis of BM cells showed that among the pod$^+$ population, the c-KIT$^+$ or VEGFR-3$^+$, but not LYVE-1$^+$, cells were more highly enriched in the tumor (melanoma)-bearing mice than in the normal mice (Figure 5B). The frequency of c-KIT$^+$ cells in the pod$^+$ population of tumor-bearing mice was 24.8±3.3%, whereas ≈16.3±2.0% of c-KIT$^+$ cells were pod$^+$ (Figure V in the online-only Data Supplement). In PB cells, among the pod$^+$ population, VEGFR-3$^+$ or LYVE-1$^+$, but not c-KIT$^+$. cells were more enriched in the tumor-bearing mice than in the normal mice. These findings suggest that during the process of lymphatic vascular growth, pod$^+$ cells not only increase in number but also undergo qualitative changes into more lymphatic and progenitor-like cells, as evidenced by an increase in VEGFR-3, LYVE-1, and c-KIT, respectively. We also observed differences between BM and PB in the composition of these markers. In BM, c-KIT expression was higher in tumor mice than normal mice; in PB, however, there was no difference in c-KIT expression between the two (Figure 5B and 5D, left). On the other hand, there was no difference in LYVE-1 expression in BM between tumor mice and normal mice, but in PB, the expression was higher in tumor mice than normal mice (Figure 5B and 5D, right). In summary, among pod$^+$ cells, c-KIT$^+$ cells were more enriched in BM and LYVE-1$^+$ cells were more enriched in PB in tumor mice compared with normal mice. Because stem/progenitor cells are more predominant in BM and undergo differentiation during mobilization into PB, these results imply that among pod$^+$ cells, progenitor forms are more prevalent in BM, and during and after mobilization into PB, the composition of pod$^+$ cells shifts to more lymphatic and less progenitor-like phenotypes. The increase in absolute percentage of VEGFR-3$^+$ cells among the pod$^+$ population in PB compared with BM further supports this interpretation (Figure 5B and 5D, middle). Finally, to determine the lymphvasculogenic potential of freshly isolated BM pod$^+$ cells in vivo, we injected the pod$^+$ cells (Dil labeled) derived from BM of tumor-bearing mice into skin and ear wound models. Immunohistochemistry showed that the injected cells were incorporated into lymphatic vessels and exhibited an LEC marker (Figure 6A and 6B). Together, these results demonstrated that pod$^+$ cells are present in BM and PB, are increased in number under lymphatic vascular growth conditions, and contribute to lymphvasculogenesis, suggesting a pathophysiological role of pod$^+$ cells as LEPCs in vivo.

Pod Is a Determining Marker to Confer Lymphatic and Progenitor Cell Properties

Because previous studies documented that tissue resident CD11b$^+$ macrophages express LEC markers and could contribute to lymphatic vessel formation,[15] we further explored the relationship between pod and CD11b in BM-MNCs using

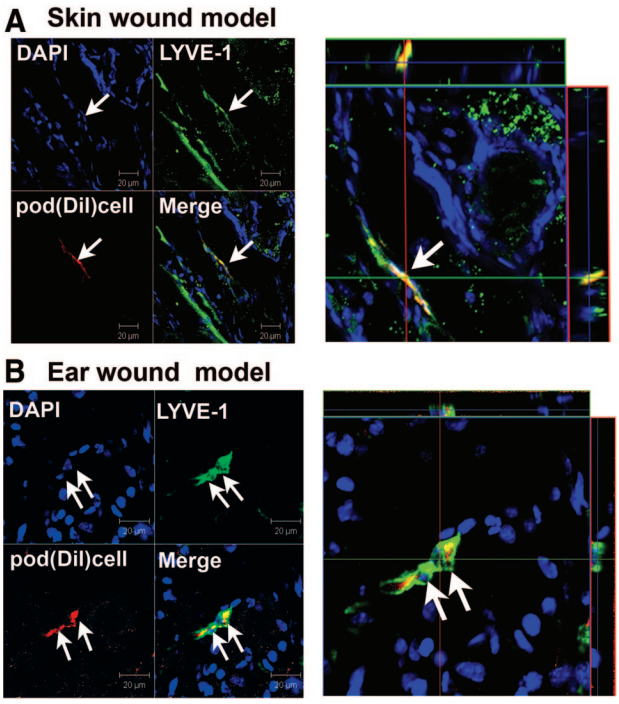

Figure 6. Incorporation of freshly isolated pod$^+$ cells into lymphatic vessels. Pod$^+$ cells isolated from BM of tumor-bearing mice were labeled with Dil and injected into mice in the skin wound (A) or ear wound (B) model. Confocal imaging showed colocalization of the injected pod$^+$ cells (red) with LYVE-1$^+$ (green) lymphatic vessels in mice. Representative images from at least 2 independent experiments for each animal model are shown (n=3 per experiment). Scale bar=20 μm.

FACS analysis. Approximately 50% of the freshly isolated BM-MNCs expressed CD11b, but <1% expressed pod (Figure 7A, left). In freshly isolated BM-MNCs, 85% of the pod$^+$ cells expressed CD11b; however, only 2% of the CD11b$^+$ cells expressed pod, showing that the majority of pod$^+$ cells express CD11b but most CD11b$^+$ cells are negative for pod. When cultured in the ACE condition for 4 days, 22% of total cells expressed pod and 62% expressed CD11b (Figure 7A, right), indicating an increase in both pod$^+$ cells and CD11b$^+$ cells but greater enrichment of pod$^+$ cells during lymphatic activation. More than 99% of these pod$^+$ cells expressed CD11b, but only 33% of CD11b$^+$ cells expressed pod, indicating that when activated by lymphangiogenic cytokines, pod$^+$ cells can virtually represent pod$^+$CD11b$^+$ cells; however, two thirds of CD11b$^+$ cells are negative for pod (Figure 7A, right). This argument is supported by the in vivo finding that the frequency of pod$^+$CD11b$^+$ cells was increased in BM of tumor-bearing mice undergoing active lymphatic neovascularization (Figure VI in the online-only Data Supplement). Together, these results suggest that during lymphatic activation, the frequency of BM cells expressing either pod or CD11b is increased, especially for cells expressing both pod and CD11b.

Next, to further define the phenotype of pod- or CD11b-expressing cells, we investigated the expression of other LEC markers (VEGFR-3 and LYVE1) and stem/progenitor markers (c-KIT and Sca-1) in each cell fraction (Figure 7B). FACS analysis showed that VEGFR-3$^+$ cells and LYVE-1$^+$ cells were present almost exclusively in the pod$^+$ population, the

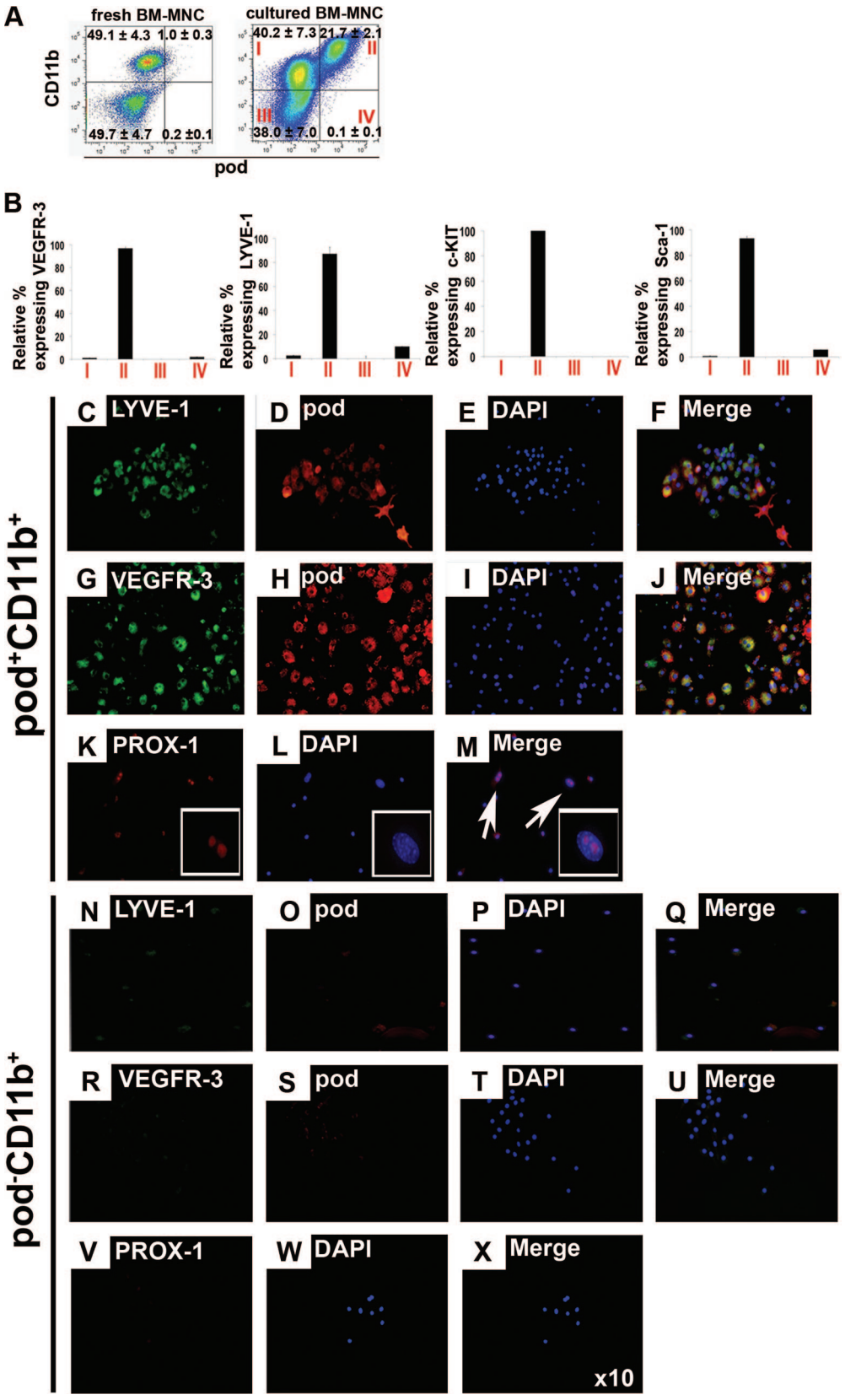

Figure 7. The relationship between pod, CD11b, stem cell markers, and LEC markers. A, The uncultured BM-MNCs or BM-MNCs cultured for 4 days were subjected to FACS analysis for pod and CD11b. Numbers in each box represent the percentages of positive cells. B, The *y* axis represents the relative percentage of cells expressing VEGFR-3, LYVE-1, c-KIT, or Sca-1 in the indicated cell fraction of A. The indicated values are the averages of 3 independent experiments (n=4 per experiment). C through X, The culture-isolated pod$^+$CD11b$^+$ or pod$^-$CD11b$^+$ cells from BM-MNCs were cultured for another 7 days under complete EGM media and stained for lymphatic markers. Representative images from at least 3 independent experiments are shown (n=4 per experiment). Magnification ×10.

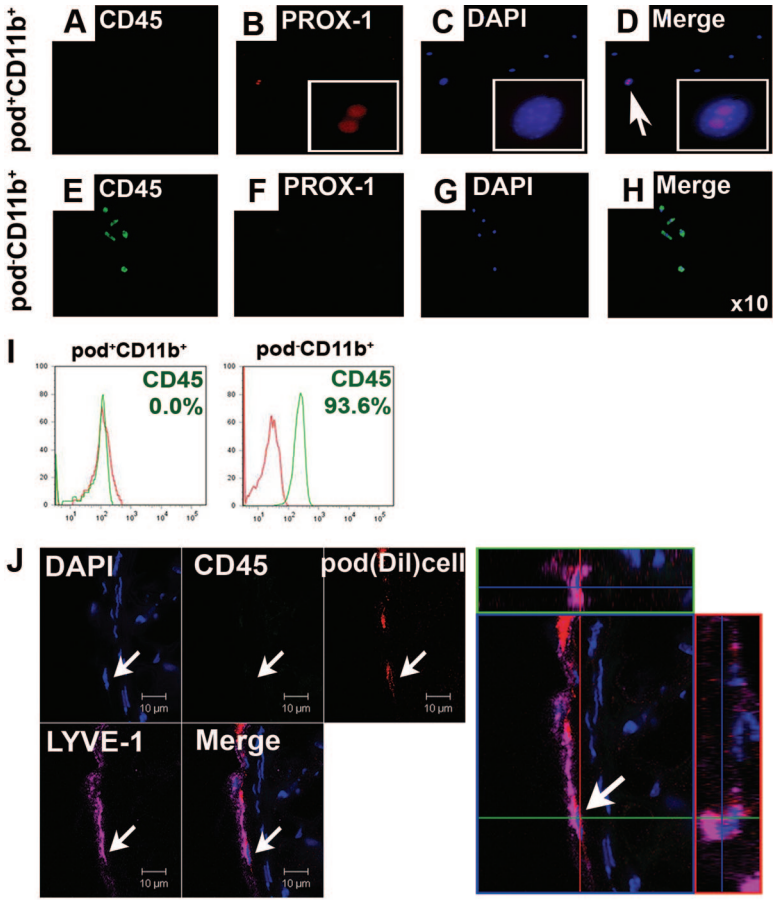

Figure 8. The pod$^+$CD11b$^+$ cells, but not pod$^-$CD11b$^+$ cells, lose expression of CD45. The culture-isolated pod$^+$CD11b$^+$ or pod$^-$CD11b$^+$ cells from BM-MNCs were further cultured for 7 days under complete EGM medium and subjected to immunocytochemistry (A through H) and FACS analysis for CD45 (I). For in vivo injection experiments (J), DiI-labeled pod$^+$CD11b$^+$ cells from the cultured BM-MNCs were injected into mice with skin wounds and subjected to immunohistochemistry (n=3 per experiment). The injected DiI-labeled cells did not express CD45 in tissues.

majority of which were pod$^+$CD11b$^+$ (fraction II in Figure 7A). These results suggest that the pod$^+$ cell population includes almost all the cells having LEC phenotypes. Approximately 99% of c-KIT$^+$ cells and 90% of Sca-1$^+$ cells were also restricted to the pod$^+$CD11b$^+$ cell fraction (Figure 7B), ie, pod$^+$ cell fraction, and only a negligible number of those cells were present in the pod$^-$CD11b$^+$ cell fraction (Figure 7A, fraction II versus I). The morphologies of the 2 cell populations were distinctively different. The pod$^+$CD11b$^+$ cells were attached and grew as a monolayer, whereas the pod$^-$CD11b$^+$ cells were floating and maintained a round cell morphology (Figure VII in the online-only Data Supplement). Importantly, when the isolated pod$^+$CD11b$^+$ or pod$^-$CD11b$^+$ cells were further cultured for 7 days in complete EGM, the pod$^+$CD11b$^+$ cells robustly expressed pod, LYVE-1, VEGFR-3, and PROX-1, whereas the pod$^-$CD11b$^+$ cells minimally expressed pod and did not express LYVE-1, VEGFR-3, or PROX-1 (Figure 7C through 7X). These data indicate that almost all the stem/progenitor cells were exclusively restricted to the pod$^+$CD11b$^+$, ie, pod$^+$, cell population. As a whole, these findings suggest that pod, more than CD11b, is a determining marker to confer lymphatic and progenitor cell properties on BM cells, robustly supporting the role of pod$^+$ cells as LEPCs.

Loss of Hematopoietic Properties of Pod$^+$CD11b$^+$ Cells During Differentiation Into LECs

We next investigated whether the hematopoietic character of the putative LEPCs or pod$^+$CD11b$^+$ cells is lost during differentiation into LECs. Pod$^+$CD11b$^+$ or pod$^-$CD11b$^+$ cells isolated from cultured BM-MNCs were further cultured for 7 days in complete EGM. Immunocytochemistry showed that pod$^+$CD11b$^+$ cells cultured for 7 days do not express CD45 while expressing LEC markers, including PROX-1 (Figures 7 and 8A through 8D). In contrast, pod$^-$CD11b$^+$ cells cultured for 7 days still maintained CD45 expression with concomitant loss of LEC markers (Figures 7 and 8E through 8H). FACS analysis additionally confirmed the loss of CD45 in the further cultured pod$^+$CD11b$^+$ cells. Approximately 94% of the pod$^-$CD11b$^+$ cells were CD45 positive (Figure 8I). To further verify these findings in vivo, we injected DiI-labeled pod$^+$CD11b$^+$ cells sorted from the cultured BM-MNCs into mice with skin wounds. Figure 8J clearly shows that expression of CD45 was not detected in the pod$^+$CD11b$^+$ cells incorporated into lymphatic vessels (Figure 8J). These data indicate that pod$^+$CD11b$^+$ cells lost hematopoietic properties during differentiation into LECs.

Discussion

This is the first study to demonstrate the presence of pod$^+$ cells in the circulatory system and to provide evidence that these cells can function as LEPCs. Pod$^+$ cells exist in BM and PB in very low amounts at steady state and increase in number under conditions that promote lymphatic vascular growth such as melanoma.[27] Pod$^+$ cells are expandable by culture with lymphangiogenic growth factors. Because lymphangiogenic tumors such as melanoma or breast cancer[28] or

inflammation[15,29] induces an increase in the local concentration of lymphatic growth factors, the cell culture conditions closely mimic the local environment of these conditions. We also successfully generated LECs in vitro by further cultivation of these culture-isolated pod$^+$ cells. Thus, this in vitro and in vivo evidence strongly suggests a crucial role for pod$^+$ cells in lymphatic vessel formation. High expression of other LEC genes and lymphangiogenic cytokines in pod$^+$ cells further supports their role in lymphatic neovascularization. The almost exclusive restriction of c-KIT, Sca-1, and FLK-1 expression to pod$^+$ cells suggests their stem/progenitor cell character.

More direct evidence of lymphatic neovascularization by pod$^+$ cells was provided by the cell injection studies. Both freshly isolated and cultured pod$^+$ cells were not only incorporated as LECs into lymphatic vasculature (lymphvasculogenesis) but also highly localized near the lymphatic vasculature, suggestive of a paracrine or lymphangiogenic role. Although there is controversy around the transdifferentiation potential of BM-derived hematopoietic cells,[30,31] our data support transdifferentiation as a viable mechanism for lymphvasculogenesis from BM cells. In fact, the prevalent view that terminally differentiated cells do not change their phenotype has been challenged.[15–17,32,33] B lymphocytes can become macrophage-like cells on overexpression of the *C/EBP* transcription factor.[34] Fully differentiated somatic cells can be reprogrammed into pluripotent stem cells with ectopic expression of pluripotency-related transcription factors.[35] A battery of 3 transcription factors was able to convert differentiated exocrine cells into functional β-cells in adult mice.[36] Conditional inactivation of *Prox1* in adult mice induced cell fate change from LECs into blood endothelial cells,[25] suggesting plasticity of differentiated cells. Our data also showed that BM-derived pod$^+$ cells clearly express PROX-1 and could become LECs in pathological conditions. To determine the contribution of injected pod$^+$ cells to LECs, we used comprehensive and multimodal approaches. Both freshly isolated and culture-isolated pod$^+$ cells were used as cell sources. For cell tracking in vivo, both DiI-labeled and GFP-mice–derived cells were used. As in vivo models, we used various animal models such as tumor, inflammation, and wound models, which represent the most prevalent clinical conditions associated with lymphatic vascular growth. The fact that pod$^+$ cells gave rise to LECs in all these models supports the identity of pod$^+$ cells as LEPCs. To prove this transdifferentiation, we used both static and in vivo confocal microscopy technologies and adopted rigorous criteria as follows. As criteria for transdifferentiation, we required not only the incorporation of injected cells into lymphatic vessels but also exact colocalization of injected cells showing single nuclei with LEC marker staining at 2 different orthogonal images and at multiple Z-stacked files. To further confirm this colocalization, 3-dimensional reconstructions were used. In addition, for identification of lymphatic vessels that harbor the injected cells, both positive staining for multiple lymphatic markers and clear morphology of the vessels were required. These multiple criteria and high standards ensured that we were seeing true transdifferentiation of injected cells rather than artifacts. Common expression of LYVE-1 in LECs and a subpopulation of monocyte-macrophage lineage increases this likelihood of transdifferentiation as well.[15,37,38]

Our data indicate that pod$^+$ cells also contribute to lymphatic neovascularization through paracrine lymphangiogenic effects on existing lymphatic vessels. Similar evidence for the role of BM-derived cells in postnatal lymphangiogenesis in pathological conditions has been reported. He et al[9] showed that BM-derived GFP$^+$ cells were heavily recruited to the periphery of new lymphatic vessels after tumor implantation, although a few were incorporated into lymphatic vessels. In other reports, depletion of macrophages inhibited inflammation-induced new lymphatic vessel formation.[29,39] Macrophages isolated from mice undergoing extensive lymphangiogenesis displayed a marked increase in lymphangiogenic cytokines.[39,40] These studies support a specific population of BM-derived cells playing an important role in lymphangiogenesis.

In this study, we demonstrated that BM cells that express pod and CD11b can function as LEPCs. A recent report showed that CD11b$^+$ macrophages may play an important role in inflammation-induced lymphvasculogenesis in the cornea.[15] However, this study demonstrated only that tissue-resident CD11b$^+$ macrophages, which are presumably derived from BM, show an LEC phenotype. In contrast, our study clearly demonstrated that BM hematopoietic cells are the source of lymphvasculogenic CD11b$^+$ cells and, using in vitro culture methods and in vivo physiological and pathological conditions, further identified a specific cell population among the heterogeneous CD11b$^+$, ie, pod$^+$CD11b$^+$, cells that can function as LEPCs.

Our study identifies pod$^+$ cells as LEPCs and proposes their crucial role in lymphvasculogenesis and lymphangiogenesis. The identification of this phenotype has important clinical significance. A culture isolation protocol has been established, so these cells can be used for treating diseases that can benefit from a lymphatic vascular supply such as lymphedema or wound healing. Furthermore, the quantification of these cells in BM may be used to measure or predict tumor burden, progression, or metastasis, allowing their use as a biomarker.

Acknowledgments

We would like to thank Debby Martinson for confocal imaging, Mackenzie Houge and Min-Young Lee for technical assistance, Andrea Wecker for critical reading of the manuscript, and Dr Mejeong Lee for support for the initial steps of this project.

Sources of Funding

This work was supported in part by an Idea Grant Award from the Department of Defense (W81XWH-09-1-0278); National Institutes of Health grants (RO1HL084471, R21HL097353); a Public Health Services grant (UL1 RR025008) from the Clinical and Translational Science Award Program, National Institutes of Health, National Center for Research Resources; and a grant (SC4300) from the Stem Cell Research Center of the 21st Century Frontier Research Program funded by the Ministry of Science and Technology, Republic of Korea.

Disclosures

None.

References

1. Achen MG, McColl BK, Stacker SA. Focus on lymphangiogenesis in tumor metastasis. *Cancer Cell*. 2005;7:121–127.
2. Alitalo K, Tammela T, Petrova TV. Lymphangiogenesis in development and human disease. *Nature*. 2005;438:946–953.
3. Wigle JT, Oliver G. Prox1 function is required for the development of the murine lymphatic system. *Cell*. 1999;98:769–778.
4. Kaipainen A, Korhonen J, Mustonen T, van Hinsbergh VW, Fang GH, Dumont D, Breitman M, Alitalo K. Expression of the fms-like tyrosine kinase 4 gene becomes restricted to lymphatic endothelium during development. *Proc Natl Acad Sci U S A*. 1995;92:3566–3570.
5. Banerji S, Ni J, Wang SX, Clasper S, Su J, Tammi R, Jones M, Jackson DG. LYVE-1, a new homologue of the CD44 glycoprotein, is a lymph-specific receptor for hyaluronan. *J Cell Biol*. 1999;144:789–801.
6. Wetterwald A, Hoffstetter W, Cecchini MG, Lanske B, Wagner C, Fleisch H, Atkinson M. Characterization and cloning of the E11 antigen, a marker expressed by rat osteoblasts and osteocytes. *Bone*. 1996;18:125–132.
7. Breiteneder-Geleff S, Soleiman A, Kowalski H, Horvat R, Amann G, Kriehuber E, Diem K, Weninger W, Tschachler E, Alitalo K, Kerjaschki D. Angiosarcomas express mixed endothelial phenotypes of blood and lymphatic capillaries: podoplanin as a specific marker for lymphatic endothelium. *Am J Pathol*. 1999;154:385–394.
8. Schacht V, Ramirez MI, Hong YK, Hirakawa S, Feng D, Harvey N, Williams M, Dvorak AM, Dvorak HF, Oliver G, Detmar M. T1alpha/podoplanin deficiency disrupts normal lymphatic vasculature formation and causes lymphedema. *EMBO J*. 2003;22:3546–3556.
9. He Y, Rajantie I, Ilmonen M, Makinen T, Karkkainen MJ, Haiko P, Salven P, Alitalo K. Preexisting lymphatic endothelium but not endothelial progenitor cells are essential for tumor lymphangiogenesis and lymphatic metastasis. *Cancer Res*. 2004;64:3737–3740.
10. Karpanen T, Egeblad M, Karkkainen MJ, Kubo H, Yla-Herttuala S, Jaattela M, Alitalo K. Vascular endothelial growth factor C promotes tumor lymphangiogenesis and intralymphatic tumor growth. *Cancer Res*. 2001;61:1786–1790.
11. Karkkainen MJ, Haiko P, Sainio K, Partanen J, Taipale J, Petrova TV, Jeltsch M, Jackson DG, Talikka M, Rauvala H, Betsholtz C, Alitalo K. Vascular endothelial growth factor C is required for sprouting of the first lymphatic vessels from embryonic veins. *Nat Immunol*. 2004;5:74–80.
12. Nagy JA, Vasile E, Feng D, Sundberg C, Brown LF, Detmar MJ, Lawitts JA, Benjamin L, Tan X, Manseau EJ, Dvorak AM, Dvorak HF. Vascular permeability factor/vascular endothelial growth factor induces lymphangiogenesis as well as angiogenesis. *J Exp Med*. 2002;196:1497–1506.
13. Cao R, Bjorndahl MA, Gallego MI, Chen S, Religa P, Hansen AJ, Cao Y. Hepatocyte growth factor is a lymphangiogenic factor with an indirect mechanism of action. *Blood*. 2006;107:3531–3536.
14. Salven P, Mustjoki S, Alitalo R, Alitalo K, Rafii S. VEGFR-3 and CD133 identify a population of CD34+ lymphatic/vascular endothelial precursor cells. *Blood*. 2003;101:168–172.
15. Maruyama K, Ii M, Cursiefen C, Jackson DG, Keino H, Tomita M, Van Rooijen N, Takenaka H, D'Amore PA, Stein-Streilein J, Losordo DW, Streilein JW. Inflammation-induced lymphangiogenesis in the cornea arises from CD11b-positive macrophages. *J Clin Invest*. 2005;115:2363–2372.
16. Religa P, Cao R, Bjorndahl M, Zhou Z, Zhu Z, Cao Y. Presence of bone marrow-derived circulating progenitor endothelial cells in the newly formed lymphatic vessels. *Blood*. 2005;106:4184–4190.
17. Kerjaschki D, Huttary N, Raab I, Regele H, Bojarski-Nagy K, Bartel G, Krober SM, Greinix H, Rosenmaier A, Karlhofer F, Wick N, Mazal PR. Lymphatic endothelial progenitor cells contribute to de novo lymphangiogenesis in human renal transplants. *Nat Med*. 2006;12:230–234.
18. Kenyon BM, Voest EE, Chen CC, Flynn E, Folkman J, D'Amato RJ. A model of angiogenesis in the mouse cornea. *Invest Ophthalmol Vis Sci*. 1996;37:1625–1632.
19. Yoon YS, Murayama T, Gravereaux E, Tkebuchava T, Silver M, Curry C, Wecker A, Kirchmair R, Hu CS, Kearney M, Ashare A, Jackson DG, Kubo H, Isner JM, Losordo DW. VEGF-C gene therapy augments postnatal lymphangiogenesis and ameliorates secondary lymphedema. *J Clin Invest*. 2003;111:717–725.
20. Hong YK, Lange-Asschenfeldt B, Velasco P, Hirakawa S, Kunstfeld R, Brown LF, Bohlen P, Senger DR, Detmar M. VEGF-A promotes tissue repair-associated lymphatic vessel formation via VEGFR-2 and the alpha1beta1 and alpha2beta1 integrins. *FASEB J*. 2004;18:1111–1113.
21. Deasy BM, Qu-Peterson Z, Greenberger JS, Huard J. Mechanisms of muscle stem cell expansion with cytokines. *Stem Cells*. 2002;20:50–60.
22. Ledgerwood LG, Lal G, Zhang N, Garin A, Esses SJ, Ginhoux F, Merad M, Peche H, Lira SA, Ding Y, Yang Y, He X, Schuchman EH, Allende ML, Ochando JC, Bromberg JS. The sphingosine 1-phosphate receptor 1 causes tissue retention by inhibiting the entry of peripheral tissue T lymphocytes into afferent lymphatics. *Nat Immunol*. 2008;9:42–53.
23. Skobe M, Hawighorst T, Jackson DG, Prevo R, Janes L, Velasco P, Riccardi L, Alitalo K, Claffey K, Detmar M. Induction of tumor lymphangiogenesis by VEGF-C promotes breast cancer metastasis. *Nat Med*. 2001;7:192–198.
24. Stacker SA, Caesar C, Baldwin ME, Thornton GE, Williams RA, Prevo R, Jackson DG, Nishikawa S, Kubo H, Achen MG. VEGF-D promotes the metastatic spread of tumor cells via the lymphatics. *Nat Med*. 2001;7:186–191.
25. Johnson NC, Dillard ME, Baluk P, McDonald DM, Harvey NL, Frase SL, Oliver G. Lymphatic endothelial cell identity is reversible and its maintenance requires Prox1 activity. *Genes Dev*. 2008;22:3282–3291.
26. Maruyama K, Asai J, Ii M, Thorne T, Losordo DW, D'Amore PA. Decreased macrophage number and activation lead to reduced lymphatic vessel formation and contribute to impaired diabetic wound healing. *Am J Pathol*. 2007;170:1178–1191.
27. Padera TP, Kadambi A, di Tomaso E, Carreira CM, Brown EB, Boucher Y, Choi NC, Mathisen D, Wain J, Mark EJ, Munn LL, Jain RK. Lymphatic metastasis in the absence of functional intratumor lymphatics. *Science*. 2002;296:1883–1886.
28. Olmeda D, Moreno-Bueno G, Flores JM, Fabra A, Portillo F, Cano A. SNAI1 is required for tumor growth and lymph node metastasis of human breast carcinoma MDA-MB-231 cells. *Cancer Res*. 2007;67:11721–11731.
29. Cursiefen C, Chen L, Borges LP, Jackson D, Cao J, Radziejewski C, D'Amore PA, Dana MR, Wiegand SJ, Streilein JW. VEGF-A stimulates lymphangiogenesis and hemangiogenesis in inflammatory neovascularization via macrophage recruitment. *J Clin Invest*. 2004;113:1040–1050.
30. Wagers AJ, Sherwood RI, Christensen JL, Weissman IL. Little evidence for developmental plasticity of adult hematopoietic stem cells. *Science*. 2002;297:2256–2259.
31. Murry CE, Soonpaa MH, Reinecke H, Nakajima H, Nakajima HO, Rubart M, Pasumarthi KB, Virag JI, Bartelmez SH, Poppa V, Bradford G, Dowell JD, Williams DA, Field LJ. Haematopoietic stem cells do not transdifferentiate into cardiac myocytes in myocardial infarcts. *Nature*. 2004;428:664–668.
32. Gao D, Nolan DJ, Mellick AS, Bambino K, McDonnell K, Mittal V. Endothelial progenitor cells control the angiogenic switch in mouse lung metastasis. *Science*. 2008;319:195–198.
33. Purhonen S, Palm J, Rossi D, Kaskenpaa N, Rajantie I, Yla-Herttuala S, Alitalo K, Weissman IL, Salven P. Bone marrow-derived circulating endothelial precursors do not contribute to vascular endothelium and are not needed for tumor growth. *Proc Natl Acad Sci U S A*. 2008;105:6620–6625.
34. Xie H, Ye M, Feng R, Graf T. Stepwise reprogramming of B cells into macrophages. *Cell*. 2004;117:663–676.
35. Takahashi K, Tanabe K, Ohnuki M, Narita M, Ichisaka T, Tomoda K, Yamanaka S. Induction of pluripotent stem cells from adult human fibroblasts by defined factors. *Cell*. 2007;131:861–872.
36. Zhou Q, Brown J, Kanarek A, Rajagopal J, Melton DA. In vivo reprogramming of adult pancreatic exocrine cells to beta-cells. *Nature*. 2008;455:627–632.
37. Schledzewski K, Falkowski M, Moldenhauer G, Metharom P, Kzhyshkowska J, Ganss R, Demory A, Falkowska-Hansen B, Kurzen H, Ugurel S, Geginat G, Arnold B, Goerdt S. Lymphatic endothelium-specific hyaluronan receptor LYVE-1 is expressed by stabilin-1+, F4/80+, CD11b+ macrophages in malignant tumours and wound healing tissue in vivo and in bone marrow cultures in vitro: implications for the assessment of lymphangiogenesis. *J Pathol*. 2006;209:67–77.

38. Cho HJ, Lee N, Lee JY, Choi YJ, Ii M, Wecker A, Jeong JO, Curry C, Qin G, Yoon YS. Role of host tissues for sustained humoral effects after endothelial progenitor cell transplantation into the ischemic heart. *J Exp Med*. 2007;204:3257–3269.
39. Kataru RP, Jung K, Jang C, Yang H, Schwendener RA, Baik JE, Han SH, Alitalo K, Koh GY. Critical role of CD11b+ macrophages and VEGF in inflammatory lymphangiogenesis, antigen clearance, and inflammation resolution. *Blood*. 2009;113:5650–5659.
40. Jeon BH, Jang C, Han J, Kataru RP, Piao L, Jung K, Cha HJ, Schwendener RA, Jang KY, Kim KS, Alitalo K, Koh GY. Profound but dysfunctional lymphangiogenesis via vascular endothelial growth factor ligands from CD11b+ macrophages in advanced ovarian cancer. *Cancer Res*. 2008;68:1100–1109.

CLINICAL PERSPECTIVE

In this study, we identified podoplanin-expressing lymphatic endothelial progenitor cells derived from bone marrow. Injection of these podoplanin-expressing lymphatic endothelial progenitor cells into various animal models showed the contribution of these cells to the formation of new lymphatic vessels through direct transdifferentiation and paracrine effects. This lymphatic vessel–forming capability can be used for the treatment of lymphedema or chronic unhealed wounds, which are characterized by lymphatic vascular insufficiency. Moreover, this study demonstrated an increase in the number of circulating lymphatic endothelial progenitor cells in tumor-bearing mice, suggesting that lymphatic endothelial progenitor cells are correlated with tumor-associated lymphatic vascular growth. This property can be harnessed for the development of a biomarker for monitoring tumor burden, tumor growth, and/or metastasis.

SUPPLEMENTAL MATERIAL

Ji Yoon Lee, Changwon Park, Yong Pil Cho, Eugine Lee, Hyongbum Kim, Pilhan Kim, Seok H. Yun, and Young-sup Yoon

Podoplanin-expressing Cells Derived from Bone Marrow Play a Crucial Role in Postnatal Lymphatic Neovascularization

Supplemental Methods

All protocols for animal experiments were approved by the Institutional Animal Care and Use Committees of Emory University.

Culture of BM-MNCs and SVEC4-10 cells

BM-MNCs were flushed from the tibias and femurs of 8-10 week old FVB mice or C57BL/6 eGFP transgenic mice (Jackson Laboratory), and fractionated by density gradient centrifugation with Histopaque®-1083 (Sigma, St. Louis, MO) to isolate mononuclear cells. Subsequently, the BM-MNCs were seeded at a density of 0.4-0.6 x $10^6/cm^2$ onto 100 mm culture dishes coated with rat plasma vitronectin (Sigma). To optimize culture conditions to generate LEPCs, four different combinations of media were employed (online-only Data Supplemental Table 1). During culture under these four conditions, non-adherent cells were discarded and only the attached cells were used for subsequent analysis and experiments. To differentiate MACS-sorted pod^+ or pod^- cells, and FACS-sorted pod^+CD11b^+ or pod^-CD11b^+ cells derived from cultured BM-MNCs into LECs, the cells were maintained in EBM-2 supplemented with 10% FBS, antibiotics, and cytokine cocktail (SingleQuots; Clonetics, Palo Alto, CA) for 7 days. The medium was changed on day 4 of the culture which was supplemented with the same cytokine cocktail. To maintain SVEC4-10 cells[1] (ATCC, CRL-2181), we used high glucose DMEM supplemented with 10% FBS and 4 mM L-glutamine adjusted to contain 1.5 g/L sodium bicarbonate.

Evaluation of plasticity of pod$^+$ cells in culture

Pod$^+$ cells isolated from 4 day-cultured BM-MNCs were cultured under the conditions supporting differentiation of each cell lineage. For endothelial cell differentiation[2], the pod$^+$ cells were plated onto vitronectin-coated dishes (1x 10^6 cells) and cultured in EGM-2 supplemented with 50 ng/ml VEGFA (R&D Systems, 293-VE-101) for 14 days. The resulting cells were stained with anti-vWF (Abcam) and anti-VE-cadherin (BD Biosciences) antibodies. For smooth muscle cell differentiation[3], we used high glucose DMEM/10% FBS with platelet-derived growth factor-BB (PDGF-BB, 10 ng/ml, Invitrogen, PHG0045). Antibodies against smooth muscle actin (Abcam, ab32575) and Desmin (Sigma, D1033) were used for immunocytochemistry. For fibroblast differentiation[4], the pod$^+$ cells were cultured in DMEM/10% FBS media, and were subjected to immunocytochemistry with anti-Vimentin (Santa Cruz, sc-7557) antibody. Secondary antibodies conjugated with Alexa 488 or Alexa 555 were used to visualize these primary antibodies.

Magnetic activated cell sorting (MACS) and fluorescence activated cell sorting (FACS)

For sorting of pod$^+$ cells with MACS, adherent cells 4 days after culture in the presence of VEGF-A, VEGF-C and EGF (all from R&D Systems, Minneapolis, MN) were trypsinized and resuspended in AutoMACS rinsing buffer. The cells were incubated with Syrian hamster anti-mouse pod antibody (Developmental Studies Hybridoma Bank, Seattle, WA) followed by biotin-conjugated goat anti-

hamster IgG antibody (Serotec, Brentwood, NH). After washing, the mixture was incubated with anti-biotin microbeads and subjected to MACS sorting (MiltenyiBiotec, Bergisch Gladbach, Germany). The same procedures were applied to sort pod^+ cells from SVEC4-10 cells. For sorting of pod^+ cells with FACS, the cultured cells or primarily isolated cells from BM of tumor bearing mice (refer to the mouse tumor model for the procedural details) were stained with FITC-conjugated Syrian hamster anti-mouse pod antibody (eBioscience, San Diego, CA) and were subjected to sorting with FACSVantageSE (Becton Dickinson, Franklin Lakes, NJ).

Quantitative RT-PCR

Total RNA and cDNA synthesis was performed as previously described[5]. Information on Taqman primer/probe sets (Biosearch Technologies, Novato, CA) used in this study is listed in online-only Data Supplemental Table 2. Relative mRNA expression of target genes was calculated with the comparative C_T method. All target genes were normalized to *Gapdh* in multiplexed reactions performed in triplicate. Differences in C_T values were calculated for each target mRNA by subtracting the mean value of *Gapdh* (relative expression = $2^{-\Delta CT}$).

Immunocytochemistry and immunohistochemistry

Immunocytochemistry and immunohistochemistry were conducted as previously described[6]. Cells were fixed with 100% methanol for 10 min at room temperature. After washing with PBS, the cells were blocked with 5% serum and subjected to

staining with primary antibodies, followed by incubation with secondary antibodies. DAPI was used for nuclear staining and the cells were visualized under a fluorescent microscope (Nikon, Melville, NY). For immunohistochemistry, samples frozen in OCT embedding medium (Sakura, Torrance, CA) were sectioned and stained with antibodies. Primary antibodies used were as follows: rabbit anti-mouse LYVE-1 (Millipore, Billerica, MA), rabbit anti-mouse PROX-1 (Millipore), rabbit anti-mouse VEGFR-3 (Santa Cruz Biotechnology Inc, CA), Syrian hamster anti-mouse pod (Developmental Studies Hybridoma Bank), rat anti-mouse CD45 (BD Biosciences). Cy2- or Cy3-conjugated goat anti-rabbit IgG (Jackson Immunoresearch Laboratories, West Grove, PA) and Cy3-conjugated goat anti-Syrian hamster IgG (Jackson Immunoresearch Laboratories) were used as secondary antibodies. The samples were examined with a Zeiss LSM 510 Meta confocal laser scanning microscope and LSM 510 Image software (CLSM, Carl Zeiss, Jena, Germany).

Flow cytometry

The FACS staining and analysis of mouse BM cells were performed as previously described[7]. Briefly, cells were resuspended with 100 µl of rinsing buffer and incubated with antibodies. After washing, the cells were analyzed with LSR II or FACScan (Becton Dickinson). As primary antibodies, we used PE-conjugated rat anti-mouse antibodies (Abs) against Sca-1, -FLK-1, -c-KIT, -CD45, or -CD11b (all from BD Biosciences), Alexa 488-conjugated hamster anti-mouse Ab against podoplanin (eBioscience), unconjugated rabbit anti-mouse Ab

against LYVE-1 (Acris, Herford, Germany) and biotin-conjugated rabbit anti-mouse Ab against VEGFR-3 (eBioscience). As a secondary Ab, biotinylated goat anti-rabbit IgG (Jackson Immunoresearch Laboratories) was used with APC-conjugated Streptavidin (eBioscience) to detect the biotinylated signals. Flow cytometric data were analyzed with FlowJo (Tree Star Inc., Ashland, OR) using appropriate controls with proper isotype-matched IgG and unstained controls.

LEC proliferation assay

The sorted pod$^+$ and pod$^-$ cells (2.5 x 10^3) from 4 day-cultured BM-MNCs were mixed with human dermal lymphatic endothelial cells (hDLECs, 1.5 x 10^4) (Cambrex), which were pre-labeled with cell tracker CM-DiI (Invitrogen), seeded onto 96 well culture plates and co-cultured in EGM media with 1% FBS. Twenty four hours later, cells were stained with Ki67 antibody (Abcam, 1:200) and counterstained with DAPI. Cells positive for DiI, Ki67 and DAPI were counted.

For statistical analysis, we counted 714 cells in the PBS control (7 fields x ~34 cells/field x 3 independent experiments), 798 cells in the pod$^+$ group (7 fields x ~38 cells/field x 3 independent experiments) and 756 cells in the pod$^-$ group (7 fields x ~36cells/field x 3 independent experiments).

Mouse Cornea Model

The mouse corneal assay was performed as previously described[8]. FVB mice (8-10 week old males) were anesthetized with an intraperitoneal injection of ketamine and xylazine. Subsequently, a micropocket was created using a

modified von Graefe knife followed by implantation of a micropellet (0.35 mm) of sucrose aluminum sulfate coated with 12% hydron (poly (2-hydroxyethyl methacrylate), Sigma) containing 250 ng of VEGF-C and 80 ng of FGF-2 into the pocket. The pellet was positioned 0.6-0.9 mm from the corneal limbus and 1 x 10^6 carbocyanine dye CM-DiI (DiI; 1.5 μg/ml; Invitrogen, Carlsbad, CA)-labeled 4-day cultured pod^+ cells were injected into the surrounding area in the cornea. Seven days after pellet implantation, eyeballs were isolated, fixed with 4% PFA, and sectioned for immunohistochemistry.

Skin and Ear Wound Models

After shaving hairs and aseptic preparation, full-thickness excisional skin wounds (one per mouse) were created on the backs or ears of the mice using 6-mm skin biopsy punches (Baker Cummins Dermatological, Livingston, NJ). Half a million pod^+ cells or pod^+ $CD11b^+$ cells labeled with DiI or derived from GFP mice in 100 μl PBS were then injected into the wound bed at four different sites around the wound. Seven days later, the wound tissues were harvested including a perimeter of 1 to 2 mm of normal skin tissue, fixed with 4% PFA, and sectioned for immunohistochemistry. To examine lymphangiogenic cytokine expression by qRT-PCR, 2 x 10^6 of pod^+ or pod^- cells from 4 day-cultured BM-MNCs in 100 μl PBS or the same volume of PBS were injected into wounded tissues of backs of diabetic C57BLKS/J-m $^{+/+}$ Leprdb (db/db, 8-10 week old) mice. Seven days later, the skin tissues were harvested and subjected to qRT-PCR.

Mouse Tumor (Melanoma) Model

First, to evaluate the in vivo contribution of pod^+ cells derived from cultured BM-MNCs to lymphatic vessel formation (Figure 3C), 2 x 10^6 tumor cells (B16-F1 melanoma cell line) in 100 µl PBS were subcutaneously injected into the middle dorsum of C57BL/6 mice. Seven days later, when the primary tumors had reached the size of 1 cm in diameter, Dil-labeled pod^+ cells isolated from cultured BM-MNCs were injected into the tumor vicinity and the mice were sacrificed 7 days later. Second, to analyze the presence of pod^+ cells in BM and peripheral blood (PB) and pod^+CD11b^+ cells in BM (Figure 5A, 5C, online-only Data Supplemental Figure S5 and S6), FACS analysis was performed on BM-MNCs or PB-MNCs obtained from mice which had received the tumor cells 7 days before. Third, to determine the lymphvasculogenic potential of freshly isolated pod^+ cells from tumor bearing mice (Figure 6A and 6B), B16-F1 melanoma cells were injected into the backs of C57BL/6 mice for tumor induction and 7 days later, pod^+ cells were isolated from BM-MNCs of these mice using FACS, labeled with Dil and injected into mouse wound models. Seven days later, the mice were sacrificed and subjected to immunohistochemistry as described above.

In vivo confocal microscopy

We used a custom-made laser scanning confocal microscopy system that is housed in Wellman Center for Photomedicine at Harvard Medical School, as previously described[9], to track pod^+ cells and monitor LECs in vivo in live mice. An ear wound model and a corneal micropocket model were created as

described above and 1 x 10^6 pod^+ cells labeled with DiI were injected into the wound bed. After 7 days, mice were anesthetized by an intraperitoneal injection of ketamine and xylazine and placed on the heated plate on the motorized stage. Cy5.5-conjugated mouse anti-LYVE-1 antibody was intradermally injected to stain LECs in vivo. Fluorescence signals of DiI and Cy5.5 were detected after excitation with a 532 nm continuous wave (CW) laser (Cobalt, Stockholm, Sweden) and a 635 nm CW laser (Coherent, Inc., Santa Clara, CA), respectively through a 579 ± 17 nm and a 692 ± 20 nm band pass filter (Semrock, Inc., Rochester, NY), respectively.

Measurement of lymphatic capillary density

After implantation of tumors (melanomas) and injection of pod^+ or pod^- cells or the same volume of PBS as described above, tumors and surrounding peritumoral tissues including skin were harvested and subjected to immunohistochemistry with a VEGFR-3 antibody for lymphatic vessel staining[6]. Lymphatic capillary density (number of VEGFR-3^+ lymphatic vessels) was calculated from at least 10 randomly selected fields.

Statistical Analysis

Statistical analyses were performed with the Mann-Whitney U test for comparisons between two groups and the Kruskal-Wallis ANOVA test for more than two groups. Hence, the statistical analysis for Figure 2A, 2B, 2C, Figure 5 and Online Supplemental Figure S6 was performed with the Mann-Whitney U

test and the analysis for Figure 4C, E and F with the Kruskal-Wallis ANOVA test. GraphPad Prism 4 (Graph-Pad Prism, GraphPad Software Inc, SanDiego) was used for the analyses. *P* values < 0.05 were considered to denote statistical significance.

Online supplemental material

Online-only Data Supplemental Figure 1 shows the expression level of LEC markers in pod$^+$ cells and SVEC4-10 cells. Online-only Data Supplemental Figure 2 shows plasticity of pod$^+$ cells from BM-MNCs. Online-only Data Supplemental Figure 3 shows incorporation of injected pod$^+$ cells in pod$^+$ lymphatic endothelium. Online-only Data Supplemental Figure 4 describes engraftment of pod$^+$ cells adjacent to lymphatic vessels. Online-only Data Supplemental Figure 5 shows expression of podoplanin in c-KIT$^+$ cells of BM-MNCs of tumor bearing mice. Online-only Data Supplemental Figure 6 shows that the frequency of pod$^+$cD11b$^+$ cells increases in BM of tumor bearing mice. Online-only Data Supplemental Figure 7 shows comparison of morphology between pod$^+$CD11b$^+$ cells and pod$^-$CD11b$^+$ cells. Online-only Data Supplemental Video 1 and 2 show the projection view of the confocal images of Figure 3C and 3E, respectively. Online-only Data Supplemental Table 1 shows the culture conditions for LEPCs. Online-only Data Supplemental Table 2 describes the mouse-specific primers and probes for qRT-PCR.

Supplemental Figures

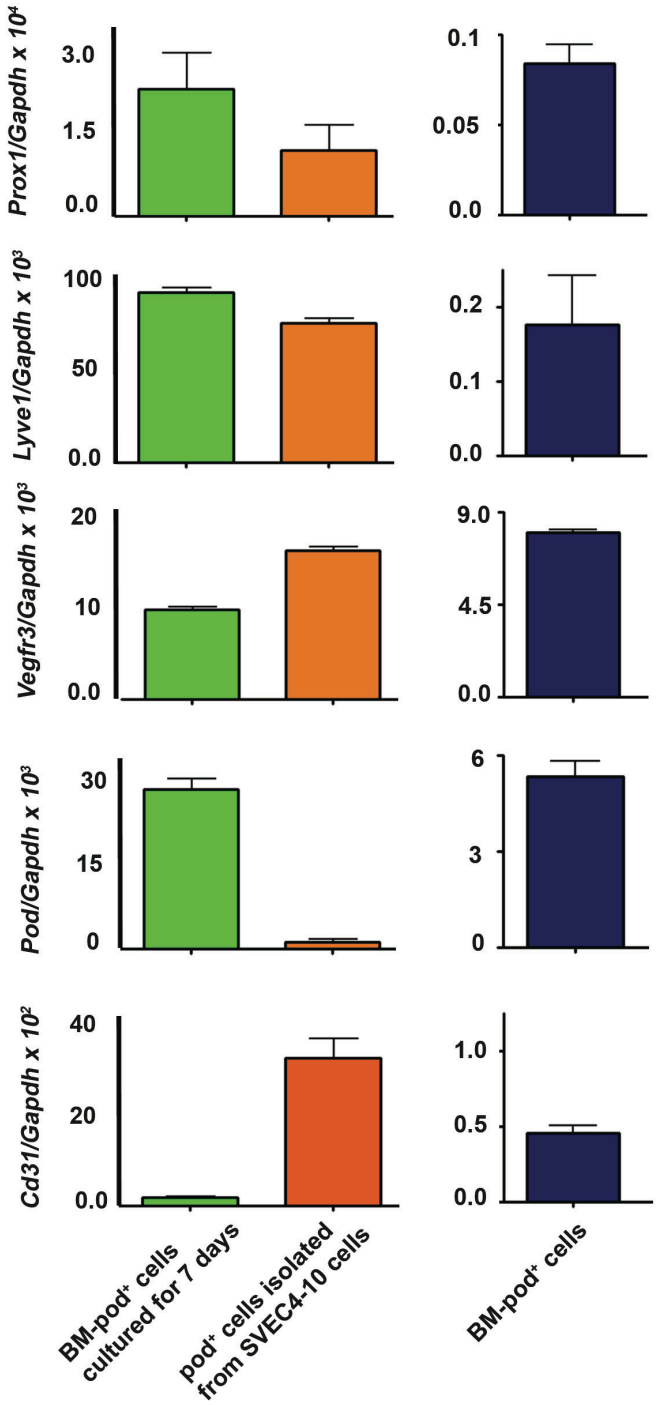

Supplemental Figure 1. The expression of LEC markers in pod$^+$ cells from BM-MNCs and SVEC4-10 cells. Pod$^+$ cells derived from BM-MNCs and SVEC4-10 cells were subjected to qRT-PCR analyses. BM-Pod$^+$: pod$^+$ cells MACS-isolated from 4 day-

cultured BM-MNCs, BM-pod$^+$ cells cultured for 7 days: pod$^+$ cells MACS-sorted from 4 day-cultured BM-MNCs and cultured for another 7 days. Graphs were presented as mean ± SE from three independent experiments.

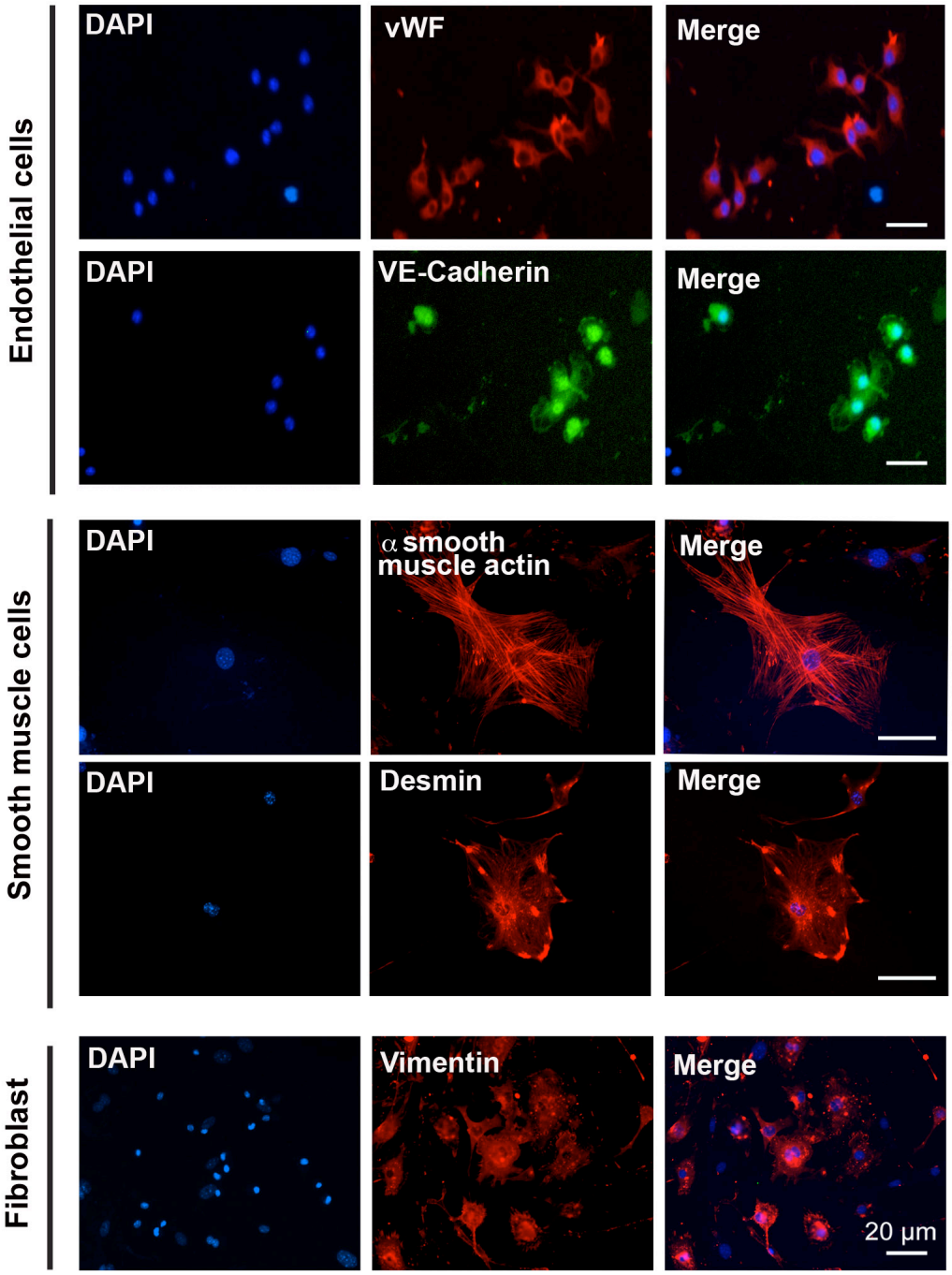

Supplemental Figure 2. BM-MNC-derived pod$^+$ cells can differentiate into endothelial cells, smooth muscle cells and fibroblasts. Pod$^+$ cells from 4 day-

cultured BM-MNCs were further cultured under the various differentiation conditions for indicated cell lineages. The resulting cells were immunostained with each lineage markers. Representative images from three independent experiments are shown. vWF; von Willebrand Factor. Scale bar = 20 um

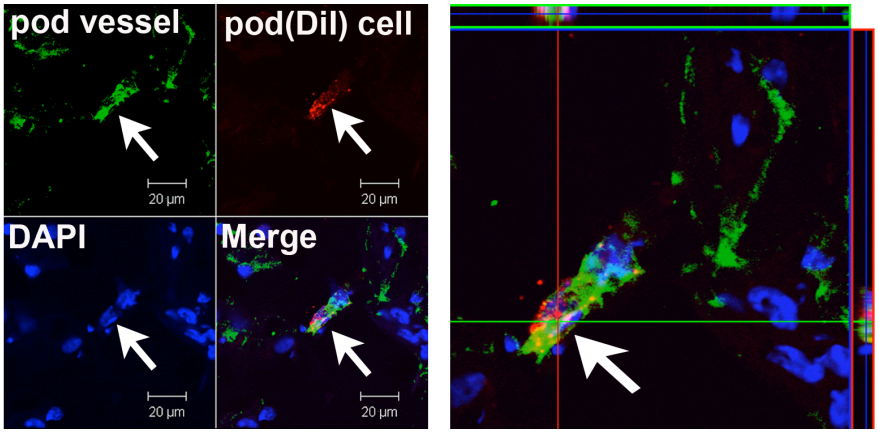

Supplemental Figure 3. Lymphvasculogenesis by the injected pod$^+$ cells in a mouse ear wound model. Mice that had received ear wound surgery were injected with DiI-labeled, pod$^+$ cells (red). Seven days later, ear tissues from the mice were harvested and sectioned for immunostaining for podoplanin (green, pod vessel). The arrow indicates incorporation of pod$^+$ cells within lymphatic vessels stained positive for podoplanin. DAPI (blue) for nuclei staining. Representative images from at least two independent experiments are shown. n=3 per experiment. Scale bar = 20 μm.

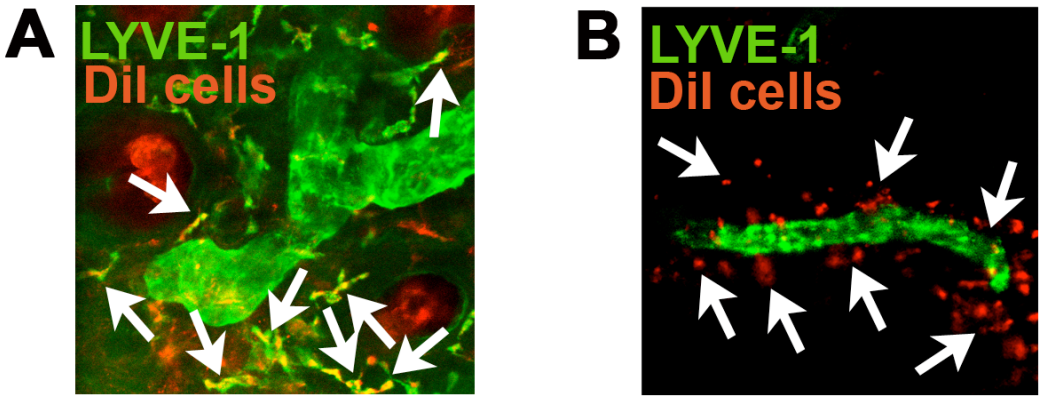

Supplemental Figure 4. Engraftment of pod$^+$ cells in lymphatic vessels. The sorted cells from the BM-MNCs were injected into mice. Seven days later, ear (A) and cornea tissues (B) from the mice were subjected to whole-mount immunostaining for podoplanin (red) and LYVE-1 (green). The arrows indicate engraftment of pod$^+$ cells adjacent to lymphatic vessels. Representative images from at least two independent experiments are shown. n=3 per experiment.

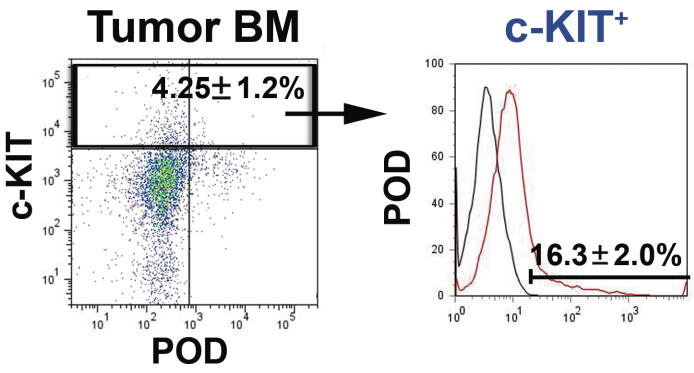

Supplemental Figure 5. Expression of Podoplanin in c-KIT$^+$ cells of BM-MNCs of tumor bearing mice. BM-MNCs of tumor (B16-F1 melanoma cells) bearing mice were subjected to FACS analysis for c-KIT and pod expression. Percentages were presented as mean ± SE from three independent experiments.

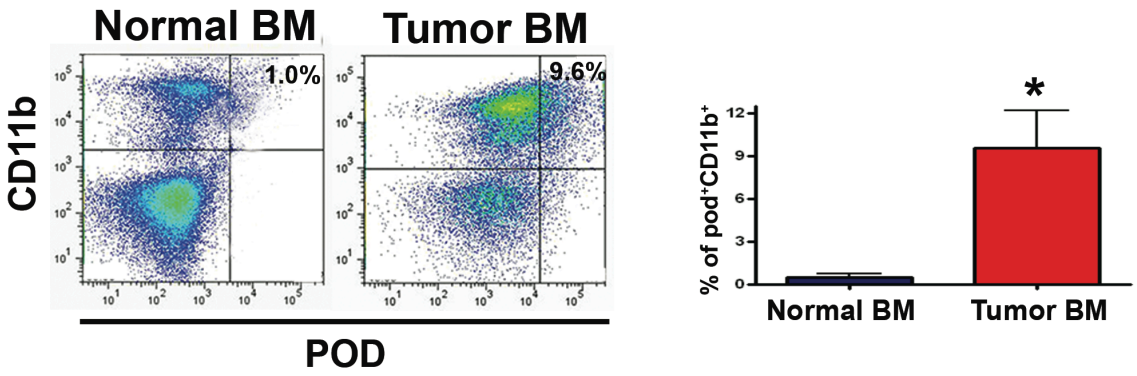

Supplemental Figure 6. The frequency of pod$^+$CD11b$^+$ cells increases in BM of tumor bearing mice. BM-MNCs harvested from mice that had been injected with B16-F1 Melanoma cells were subjected to FACS analyses for pod and CD11b expression. Graphs were presented as mean ± SE from three independent experiments (n=3 per experiment, * $P < 0.05$)

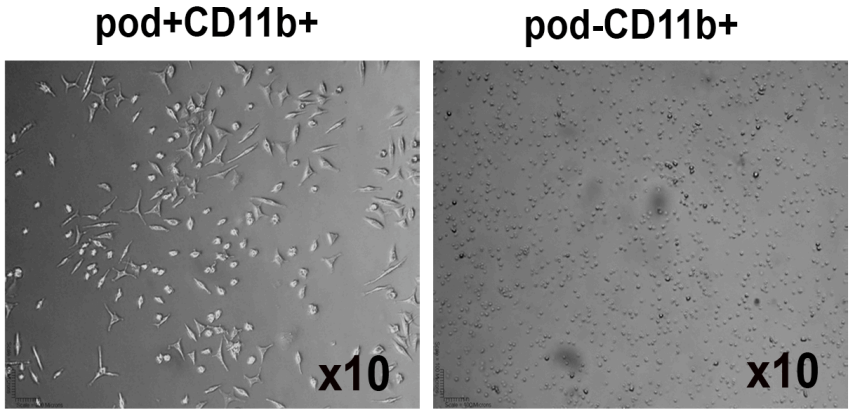

Supplemental Figure 7. Comparison of morphology between pod^{+}CD11b^{+} cells and pod^{-}CD11b^{+} cells. The sorted cells from the BM-MNCs were seeded on vitronectin-coated plates in EGM, cultured for 24 hours and monitored under an inverted microscope. The pod^{+}CD11b^{+} cells were attached as a monolayer and displayed round cobblestone- and spindle-shaped morphologies, whereas the pod^{-}CD11b^{+} cells were floating and maintained small round shape morphology. Magnification, x 10.

Supplemental Tables

Table S1. Culture conditions for LEPCs

	A	C	AC	ACE
5% FBS	+	+	+	+
VEGF-A (50 ng/ml)	+		+	+
VEGF-C (100 ng/ml)		+	+	+
EGF (10 ng/ml)				+
Ascorbic acid (100 ng/ml)	+	+	+	+

A, VEGF-A; C, VEGF-C; E, EGF; EGM, EBM-2 + SingleQuots

Table S2. Primers and probes for quantitative RT- PCR

Genes	Unigene	Primers and Probes (5`-3`)	
		Forward	CTTCCGCCATCCCTTTCC
		Reverse	CCGGAGGGAGCACCTAGTG
Prox1	NM008937	Probe	CTGCCCTTGATGGCTTATCCATTTCAGA
		Forward	CAGCAGCAGCGCCTACTTG
		Reverse	CCGGGTGGTGGCAGAA
Lyve1	NM053237	Probe	TCATCCCCTGACTCCACAACACC
		Forward	TGGCAAGGCACCTCTGGTA
		Reverse	TGAGGTGGACAGTTCCTCTAAGG
pod	NM010329	Probe	CAACGCAGAGAGAGCGTGGGACG
		Forward	TGCTGAAAGAGGGCGCTACT
		Reverse	TGCCGATGTGAATTAGGATCTTG
Vegfr3	NM008029	Probe	AGCACCGTGCCCTGATGTCGGA
		Forward	TCCCCGAAGCAGCACTCTT
		Reverse	ACCGCAATGAGCCCTTTCT
Cd31	NM001032378	Probe	CAGTCAGAGTCTTCCTTGCCCCATGG
		Forward	CATCTTCAAGCCGTCCTGTGT
		Reverse	CAGGGCTTCATCGTTACAGCA
Vegfa	NM0010252503	Probe	CCGCTGATGCGCTGTGCAGG
		Forward	CAGCAAGACGTTGTTTGAAATTACA
		Reverse	GTGATTGGCAAAACTGATTGTGA
Vegfc	NM0000745	Probe	CCTCTCTCACAAGGCCCCAAACCA
		Forward	GCAAATCGCGCACTCTGA
		Reverse	TGGCAAGACTTTTGAGCTTCAA
Vegfd	NM010216	Probe	ACTGGAAGCTGTGGCGATGCCG
		Forward	TGCTTCCGGAGCTGTGATCT
		Reverse	CGGGCTGCTTTTGTAGGCT
Igf1	NM0011112741	Probe	AGGAGACTGGAGATGTACTGTGCCCCAC
		Forward	GGGCTGTGTTCCCATCCAT
		Reverse	AGGAGTCCTTCTGACCCATACCT
Ang1	NM0096403	Probe	TGGGCCGACCCCGTCACC
		Forward	GTCACGGAAATACTCCAGTTGGT
		Reverse	CCGTTTTGGATCCGAGTTTATACT
bFgf	NM0080062	Probe	TGTGGCACTGAAACGAACTGGG
		Forward	CTGACCCAAACATCCGAGTTG
		Reverse	TTCCCATTGCCACGATAACAA
Hgf	NM0104274	Probe	TGCTCTCAGATTCCCAAGTGTGACGTGT
		Forward	TGGTGTGTGACGTTCCCATT
		Reverse	CAGCACGAGGCTTTTTTGTTG
Il1	NM0083613	Probe	ACAGCTGCACTACAGGCTCCGAGATGA

		Forward	CGTGTTCCTACCCCCAATGT
		Reverse	TGTCATCATACTTGGCAGGTTTCT
Gapdh	NM001001303	Probe	TCGTGGATCTGACGTGCCGCC

Supplemental Legends for The Videos

Legend for Video 1. Representative projection view of the engrafted podoplanin$^+$ cells in a tumor model.

Mice which had been implanted with tumor cells (B16-F1 Melanoma) were injected with DiI-labeled pod$^+$ cells (red) and the tissues were harvested 7 days later for immunohistochemistry. Representative confocal images from peritumoral subcutaneous tissues demonstrated that DiI-labeled pod$^+$ cells were incorporated into lymphatic vessels and exhibited a LEC marker, LYVE-1 (green).

Legend for Video 2. Representative projection view of the engrafted podoplanin$^+$ cells in a wound model.

A skin wound model was created and the pod$^+$ cells from GFP mice were injected into peri-wound tissues. Seven days later, the tissues were harvested and immunostained for LYVE-1 (red). Confocal microscopic examination with 3D reconstruction showed that injected pod$^+$ GFP cells (arrows) were incorporated into the lymphatic vessels and expressed LYVE-1 (red).

Supplemental References

1. Ledgerwood LG, Lal G, Zhang N, Garin A, Esses SJ, Ginhoux F, Merad M, Peche H, Lira SA, Ding Y, Yang Y, He X, Schuchman EH, Allende ML, Ochando JC, Bromberg JS. The sphingosine 1-phosphate receptor 1 causes tissue retention by inhibiting the entry of peripheral tissue T lymphocytes into afferent lymphatics. Nat Immunol. 2008;9:42-53.
2. Ferreira LS, Gerecht S, Shieh HF, Watson N, Rupnick MA, Dallabrida SM, Vunjak-Novakovic G, Langer R. Vascular progenitor cells isolated from human embryonic stem cells give rise to endothelial and smooth muscle like cells and form vascular networks in vivo. Circ Res. 2007;101:286-294.
3. Ross JJ, Hong Z, Willenbring B, Zeng L, Isenberg B, Lee EH, Reyes M, Keirstead SA, Weir EK, Tranquillo RT, Verfaillie CM. Cytokine-induced differentiation of multipotent adult progenitor cells into functional smooth muscle cells. J Clin Invest. 2006;116:3139-3149.
4. Moreau JE, Chen J, Bramono DS, Volloch V, Chernoff H, Vunjak-Novakovic G, Richmond JC, Kaplan DL, Altman GH. Growth factor induced fibroblast differentiation from human bone marrow stromal cells in vitro. J Orthop Res. 2005;23:164-174.
5. Cho HJ, Lee N, Lee JY, Choi YJ, Ii M, Wecker A, Jeong JO, Curry C, Qin G, Yoon YS. Role of host tissues for sustained humoral effects after endothelial progenitor cell transplantation into the ischemic heart. J Exp Med. 2007;204:3257-3269.

6. Yoon YS, Murayama T, Gravereaux E, Tkebuchava T, Silver M, Curry C, Wecker A, Kirchmair R, Hu CS, Kearney M, Ashare A, Jackson DG, Kubo H, Isner JM, Losordo DW. VEGF-C gene therapy augments postnatal lymphangiogenesis and ameliorates secondary lymphedema. J Clin Invest. 2003;111:717-725.

7. Yoon YS, Wecker A, Heyd L, Park JS, Tkebuchava T, Kusano K, Hanley A, Scadova H, Qin G, Cha DH, Johnson KL, Aikawa R, Asahara T, Losordo DW. Clonally expanded novel multipotent stem cells from human bone marrow regenerate myocardium after myocardial infarction. J Clin Invest. 2005;115:326-338.

8. Kenyon BM, Voest EE, Chen CC, Flynn E, Folkman J, D'Amato RJ. A model of angiogenesis in the mouse cornea. Invest Ophthalmol Vis Sci. 1996;37:1625-1632.

9. Kim P, Puoris'haag M, Cote D, Lin CP, Yun SH. In vivo confocal and multiphoton microendoscopy. J Biomed Opt. 2008;13:010501.